Ur-Rehman, F., Cashell, K.A., Anguilano, L. Post-fire structural properties of hot-rolled and cold-rolled duplex stainless steel reinforcing bar. Accepted for publication in Fire Technology, April 2022.

Post-fire structural properties of hot-rolled and cold-rolled duplex stainless steel reinforcing bar

Abstract

This paper is concerned with the behaviour of duplex stainless steel reinforcing bar following exposure to elevated temperatures from a fire followed by subsequent cooling. The study focuses on duplex grade 1.4362 reinforcing bar, and includes both hot-rolled and cold-rolled variants. Grade 1.4362 duplex stainless steel reinforcement has become a popular choice for reinforced concrete owing to its excellent combination of outstanding mechanical behaviour and corrosion resistance as well as cost-effectiveness. There is no information on the post-fire performance of duplex 1.4362 reinforcing bar available, despite being necessary for an engineer that may wish to study the structural integrity of a relevant structure following a fire. To address this gap in the existing knowledge, this paper presents a detailed discussion and analysis based on a series of laboratory experiments comprising mechanical and metallurgical testing. It is shown that grade 1.4362 duplex stainless steel reinforcing bars perform unlike any other types of carbon steel or austenitic stainless steel rebars, owing to the austenite-ferrite grain boundary, and the associated instabilities. Based on the results presented in this paper, a series of recommendations are proposed for the post-fire mechanical property retention factors that can be used in assessment and design. Finally, this paper aims to highlight the potential for rehabilitation and salvage of existing reinforced concrete structures following a fire, and aid in the prevention of unnecessary demolition and replacement.

Key	
f_u	*Ultimate tensile stress*
$f_{0.2p}$	*0.2% proof stress*
ε_f	*Total strain at failure*
ε_u	*Percentage total elongation at maximum force*
E	*Modulus of elasticity*

1.0 Introduction

This paper is concerned with the behaviour of duplex stainless steel reinforcing bars following exposure to elevated temperature and subsequent cooling. Stainless steel rebars are becoming a well-accepted solution for concrete structures which are exposed to harsh environments, such as marine or industrial settings, owing to their excellent corrosion resistance. There is increasing focus on using stainless steel rebars as an alternative to traditional carbon steel bars owing to their excellent mechanical performance, long life cycle, and reduced requirements for expensive inspection and maintenance works. There are a number of different types of stainless steel rebar, including austenitic and duplex grades, and these are appropriate for a variety of applications. Austenitic stainless steel reinforcement is most commonly employed owing to its ready availability, strong resistance to corrosion and excellent mechanical properties. However, in recent years, in common with bare stainless steel sections, the use of duplex stainless steel for rebar has been steadily increasing, largely owing to its enhanced strength (yield strength of around 450 N/mm^2), excellent ductility and very good resistance to corrosion, coupled with its relative affordability.

This paper investigates the behaviour of grade 1.4362 duplex stainless steel reinforcement, which offers similar corrosion resistance and strength to austenitic grade alloys, whilst having a lower molybdenum and nickel content. Molybdenum and nickel are two of the most expensive alloying elements used in stainless steel rebars and therefore the duplex grades can offer good cost-effectiveness compared with austenitic stainless steel, which has resulted in a steady increase in demand [1]. For example, duplex stainless steel reinforcement was recently used in the Montreal Champlain Bridge which spans 3.4 km over the St Lawrence River in Canada, and is often exposed to strong winds, heavy rainfall, seasonal snowfall and the regular use of de-icing salts. To confront this harsh environment, 15,000 tonnes of grade 1.4362 rebar was used to reinforce the most crucial areas which are susceptible to corrosion, and this promotes a long-life span of 125 years with minimal maintenance requirements [2] [3]. Another example is the Chinese River Delta Crossing, an ongoing project spanning 50 km through a series of bridges and tunnels which will connect Hong Kong, Macau and mainland China. To reduce the maintenance of this megastructure, 15,000 tonnes of grade 1.4362 rebar is employed in the outer parts that are most susceptible to high chloride levels, thus ensuring a long life-span [4].

Although the performance of stainless steel rebar in marine environments is reasonably well understood and has been the subject of some research [e.g. 5-7], studies into the fire and post-fire behaviour are scarce. In fact, there is a complete absence of any data in the literature on the post-fire performance of duplex stainless steel rebar. Gardner et al. [8] investigated the elevated temperature behaviour of duplex grade 1.4362 through both isothermal and anisothermal testing on bars that were exposed to up to 1000°C. Based on the results, a series of reduction factors for the key mechanical properties were recommended as well as material models for analysis and design. In addition, the post-fire behaviour of austenitic stainless steel rebar has been studied by Rehman, et al. [9], who studied the behaviour of cold-rolled grades 1.4301, 1.4401 and 1.4436 and Felicetti, et al. [10] who studied hot-rolled and cold-rolled grade 1.4302 rebar. Tao et al. [11] examined the residual post-fire response of three types of stainless steel (i.e. austenitic, duplex and ferritic alloys) to determine their full-range stress–strain curves following exposure to elevated temperature. The duplex grades examined were grades 1.4362 and 1.4462. This work did not study reinforcing bars and the tensile test coupons were extracted from flat sheet materials and the flat parts of square hollow sections. It was shown that coupons heated to 500°C or less, experienced a negligible change in the strength properties once they returned to room temperature. Following exposure to higher temperatures, some strength deterioration occurred in the coupons. On the other hand, for the duplex stainless steel coupons heated to 800°C or more before cooling, there was a relatively small increase in residual ductility.

This paper is concerned with the post-fire behaviour of grade 1.4362 duplex stainless steel rebar. An extensive test programme was conducted to fully understand both the mechanical and metallurgical changes that occur to these bars following exposure to elevated temperature and subsequent cooling to room temperature. This data is especially relevant for the post-fire inspection and rehabilitation of structures, to minimise or even avoid the need for demolition. The paper proceeds with a brief overview of the available and relevant literature to provide context for the later sections of the paper in which the testing programme is described and the results are analysed.

2.0 Background

Stainless steel alloys are generally categorised into five families based on their composition and crystallographic structure; these are the austenitic, ferritic, duplex, martensitic and precipitation hardening grades. Of these, austenitic and duplex stainless steels are most commonly employed in structural applications, although the ferritic grades are sometimes used in appropriate applications also. The martensitic and precipitation hardening grades are rarely if ever used in construction applications, and are more commonly employed for mechanical engineering and aerospace applications, medical tools and cutting utensils.

Austenitic stainless steels are the most common type of stainless steel, accounting for 70% of all stainless steel production [12]. They offer an excellent combination of corrosion resistance, ductility, strength and toughness. Austenitic stainless steels behave very well at high temperatures and are readily weldable. The ferritic grades are cheaper than the austenitics due to a very low nickel content [13]. However, they also offer less corrosion resistance, ductility and strength than the austenitic alloys. Ferritic alloys perform well at high temperatures but are more challenging to weld compared with the austenitics.

Duplex stainless steels are also known as austenitic-ferritic stainless steels, as they contain both an austenite and ferrite phase in their crystallographic structure. They offer higher corrosion resistance and strength than austenitic stainless steels, whilst maintaining the ductility of a ferritic stainless steel. Duplex stainless steel alloys have good weldability which is advantageous for reinforcing bar which needs to be pre-assembled into reinforcement cages, such as for piles, diaphragm walls, columns and beams. Martensitic stainless steels are extremely hard alloys but have poor ductility. They are prone to cracking when welding and perform similar to conventional carbon steels at high temperatures [14] and the precipitation hardened stainless steels are similar to martensitic alloys in purpose, offering extreme hardness but somewhat better ductility. Precipitation hardened alloys respond poorly to high temperatures but offer good weldability.

Of these five stainless steel families, only the austenitic and duplex alloys are used for rebar production. The subject of this study, grade 1.4362 duplex stainless steel rebar, is an excellent choice for structures, such as bridges, where both high corrosion resistance and strength is required. The chemical composition requirements are presented in Table 1, in accordance with the guidelines given in Part 1 of EN 10088 [15]. It is noteworthy to recognise some of the constituent elements, which are influential to the structural performance:

- Chromium (Cr): a highly resistive element to corrosion through its passive self-healing capability, and the most prominent addition in any stainless steel alloy. The addition of chromium helps strengthen and soften the alloy, whilst promoting a ferritic phase.
- Nickel (Ni): the primary austenite promoter in stainless steel is an active corrosion resisting element, the addition of Nickel promotes ductile behaviour whilst hardening the alloy.
- Molybdenum (Mo): an active corrosion resisting element with fire resisting properties at elevated temperatures of up to 500°C. As with Chromium, molybdenum is a strong ferrite promotor.
- Manganese (Mn): an active deoxidizer, crucial to the manufacturing of stainless steel through its ability to provide stability from cracking and tearing during the cooling process. At base temperatures manganese is an austenite promoting element, whereas at elevated temperatures manganese will promote a ferrite phase.

Table 1 – Chemical Composition requirement of Grade 1.4362 duplex stainless steel rebar (EN 10088-1, 2014).

Grade	2304	
EN 10088-1	1.4362	
Steel Name	X2CrNiN23-4	
%wt	Min	Max
%C - Carbon	-	0.03
%Mn - Manganese	-	2
%Si - Silicon	-	1
%S - Sulfur	-	0.03
%P - Phosphorus	-	0.035
%Ni - Nickel	3.5	5.5
%Cr - Chromium	22	24.5
%Mo - Molybdenum	0.1	0.6
%N - Nitrogen	0.05	0.2
%Cu - Copper	0.1	0.6

Besides the chemical composition, another influential factor in the characteristics of the alloy is the method of production. For rebar, this can be broken down into either hot-rolling or cold-rolling. Hot-rolling the rebar is the practice of transforming the steel billet to a finished rebar in one continuous chain of actions under controlled elevated temperature conditions, then allowing for subsequent cooling. Production through cold-rolling is working the steel billet into coils of steel wire at elevated temperature, then cooling them for easier transportation and storage, as shown in Fig. 1. Following this, to form a useable product the coil is continuously drawn through rollers in a cold state to mechanically induce strength into the steel alloy. This action leads to the reduction of the diameter of the finished rebar [16].

Both methods of production have their own attributes and drawbacks which are important to consider during specification. Cold-rolling allows for better transportation and provides manufacturers and suppliers with the ability to bulk stock rebars for on-demand availability, resulting in a reduced cost of the final product but a limitation in the variation of rebar available. The ribbing on cold-rolled rebars tends to be more uniform and allows for better bond strength compared with hot-rolled bars. However, as cold-rolled rebars have to be coiled and rolled, they have a diameter limitation of between 16 and 20 mm. Hot-rolling rebars have easier workability during manufacturing and so are generally possible to produce with no diameter limitation. In addition, hot-rolled rebars are more resistant to mechanical changes following additional exposure to heat. However, due to the higher cost, hot-rolled rebar manufacturing is normally reserved for special requirements or larger diameter rebars.

Figure 1 – Cold rolled rebar coil [17]

3.0 Experimental testing

In this experimental programme, a total of 70 specimens were examined including 38 metallurgical examinations which were conducted at the Experimental Techniques Centre (ETC) at Brunel University and 32 tensile tests which were done at the Civil Engineering Laboratory, also at Brunel University. The experimental programme was designed with the aim of understanding the post-fire behaviour of both hot-rolled and cold-rolled specimens following exposure to different levels of elevated temperature as well as different cooling methods.

3.1 Materials

Both hot-rolled and cold-rolled grade 1.4362 duplex stainless steel reinforcing bars were examined, and the rebars were supplied from the same manufacturing batches. The bars were selected on the basis that were readily available from suppliers and thus representative of what would be used in a real construction project. The hot-rolled rebars had a diameter of 8 mm and the cold-rolled rebars had a diameter of 12 mm. The chemical composition provided by the manufacturers of both rebars is presented in Table 2.

Table 2 Chemical composition of the grade 1.4362 rebars

Type / Element	Hot-rolled %wt	Cold-rolled %wt
%C - Carbon	0.02	0.016
%Mn - Manganese	1.3	1.595
%Si - Silicon	0.68	0.509
%S - Sulphur	0.001	0.001
%P - Phosphorus	0.027	-
%Ni - Nickle	4.28	4.05
%Cr - Chromium	23.44	22.755
%Mo - Molybdenum	0.32	0.198
%N - Nitrogen	0.09	0.115
%Cu - Copper	0.46	0.308
%Ti- Titanium	-	0.022

In the as-received state, the mechanical properties of both the hot-rolled and cold-rolled rebar batches were tested against the mechanical requirements as set out in BS 6744:2016 [18], which is a specification for the technical requirements for stainless steel reinforcement; the results are presented in Table 3. The strength class is required to be at least equal to that of carbon steel grade B500. This means having a minimum proof strength ($f_{0.2p}$) of 480 N/mm^2, and ductility which is equal to class B (i.e. the total elongation at the maximum force (ε_u) should be ≥ 5.0%, the total elongation at failure (ε_f) should be ≥14% and the stress ratio ($f_u/f_{0.2p}$) should be ≥ 1.08).

Table 3 Mechanical requirements for Class B reinforcement [18] together with the test specimen values

	Code requirement	**Hot-rolled**	**Cold-rolled**
$f_{0.2p}$ (N/mm^2)	≥480	615.7	836.8
f_u (N/mm^2)	-	803	941.5
$f_u/f_{0.2p}$	≥1.08	1.3	1.13
ε_u (%)	≥5	16.0	1.5
ε_f (%)	≥14	21.7	19.7

The hot-rolled rebar was sourced from a UK supplier whilst the cold-rolled rebar was sourced from a European supplier. The cold-rolled rebar is not compliant with the requirements given in BS 6744 [18] as the ε_u condition of being at least 5% is not satisfied. Rodrigues et al. [16] found that a reduction of greater than 12% in the diameter leads to a change in the characteristic stress-strain response, resulting in a lower ε_u in comparison to the hot-rolled variant. The difference in the response between the two sample sets in the virgin state is presented in Fig. 2. For comparison, the idealised material response of stainless steel reinforcement is also presented in Fig. 3, highlighting the main properties which define the behaviour.

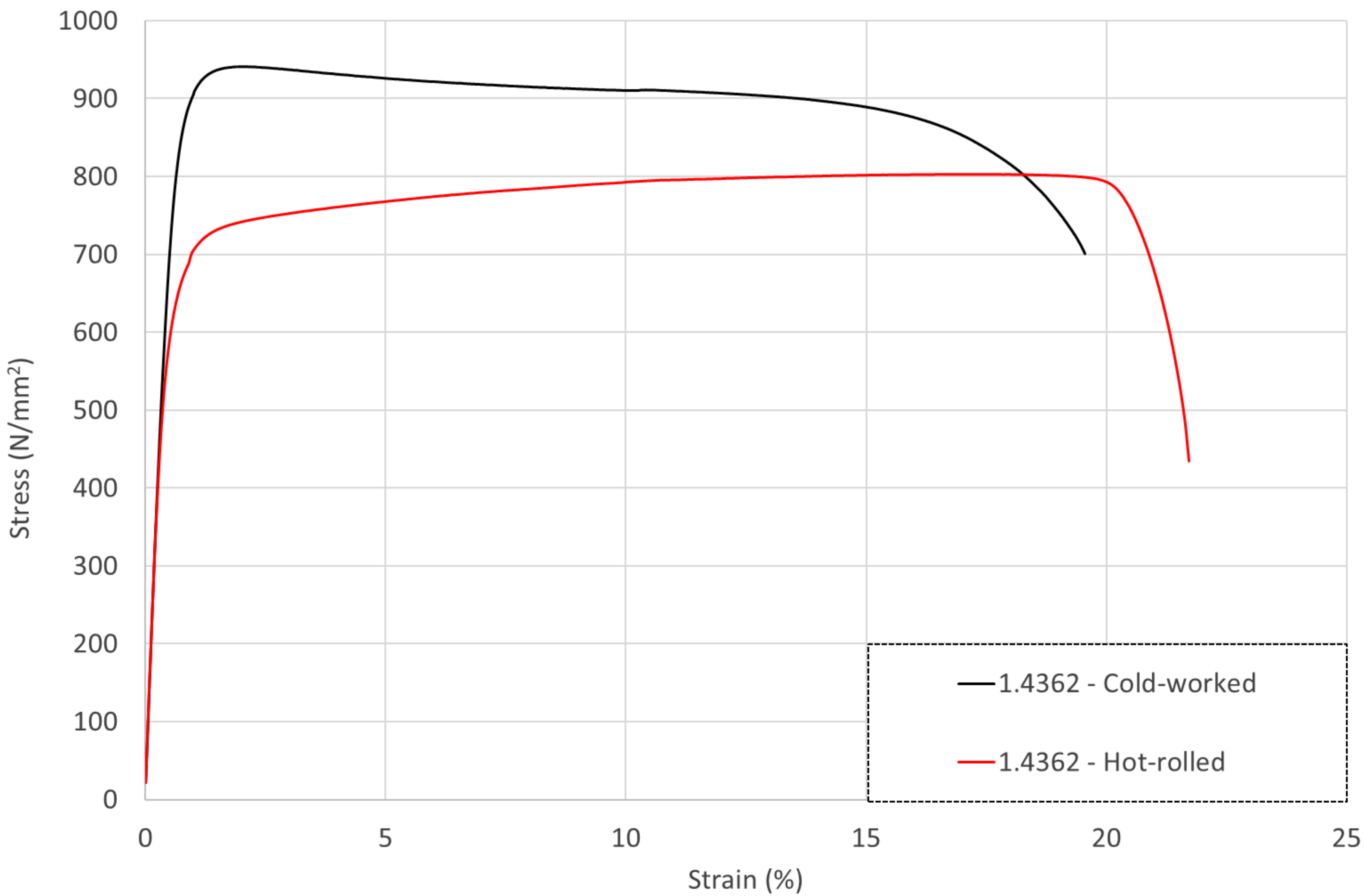

Figure 2 The stress-strain response of cold-rolled (black) versus hot-rolled (red) grade 1.4362 rebar in the as-received condition.

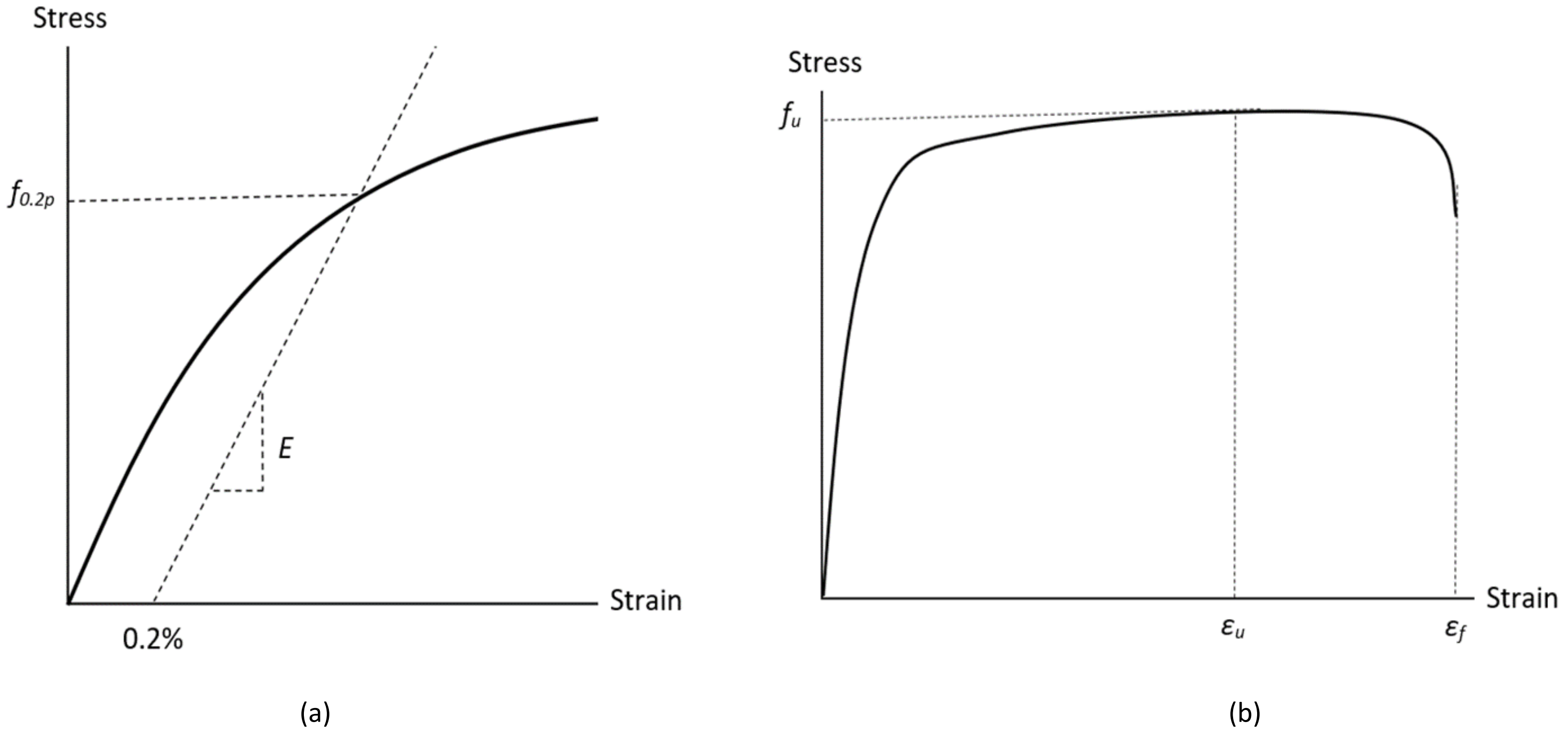

Figure 3 Idealized stress-strain response of duplex stainless steel reinforcement including (a) a focused view of the initial part of the curve and (b) the complete behavior (Adapted from [8])

3.2 Heating and cooling regime

The specimens were heated to a target temperature ranging from 500-900°C, at intervals of 100°C, in a Carbolite CWF 1100 furnace equipped with a Eurotherm 3216 control module at a rate of 10°C/min. Work done by Twilt [19] found that when heating steel, a heating rate of between 5-50°C/min may be considered realistic, with 10°C considered to be a reasonable rate for a regular fire. Although this work was focused on structural steel sections, it gives an indication of how temperature spreads through metals during a fire. Following this, the target temperature was maintained for 1 hour. The lower bound temperature of 500°C was selected as earlier studies on other grades of stainless steel [9] showed that exposure to lower temperatures had a negligible effect on the residual mechanical properties. The upper bound temperature of 900°C was selected as this is considered a realistic limit on the temperature that rebar would be exposed to, during a fire. Moreover, if the bars were exposed to higher temperatures, they would deform to such an extent that they would not retain structural integrity.

Following the heating phase of the programme, the specimens were cooled by one of three methods, in order to determine the influence that cooling rate has on the post-fire behaviour. The cooling methods were selected to replicate the range of realistic scenarios and included (i) quenching in cold water, the most rapid method of cooling, to simulate a scenario in which firefighters hose down the specimen forcing a sudden drop in temperature, (ii) natural air-cooling, which is an intermediate cooling method in terms of rate and simulates a scenario where the rebar is left exposed following a fire and allowed to cool at a natural pace and (iii) slow-cooling, a slow, controlled cooling method inside the furnace at a rate of 1°C/min, which is to replicate a scenario in which the concrete remains relatively intact and therefore the rebar is not directly exposed, allowing for slower cooling over time.

3.3 Metallurgical testing

For the material inspection, a two-part study was conducted. The first stage consisted of an X-ray diffraction (XRD) analysis, which was conducted on specimens for all examined levels of temperature exposure and cooling methods. The XRD analysis was performed using a Bruker D8 diffractometer equipped with a copper source and Lynxeye position sensitive detector, further analysis was carried out using the DIFFRAC.EVA software for phase identification.

Following this, a more detailed inspection was carried out through backscatter imaging (using a back-scattering detector BSD) within a Zeiss Crossbeam to collect the detailed grain imagery, and then Fiji ImageJ software to analyse the imagery. The purpose of the metallurgical testing programme was to develop a complete understanding of any phase transitioning, and to monitor the grain changes; these observations are then linked to the mechanical properties.

3.4 Mechanical testing

Following the heating and cooling cycles, the mechanical tensile tests were conducted at an ambient room temperature of 18°C using an Instron 5584 electromagnetic testing frame with a maximum loading capacity of 150 kN. The arrangement was equipped with an Instron EX2620-601 extensometer for the strain measurement; the complete setup is presented in Fig. 4. For the tensile testing, the programme followed guidance as given in BS EN ISO 6892-1:2016 [20]. Accordingly, the sample had a total length (L_t) of 150 mm, a gauge length (L_o) of 50 mm and a parallel length (L_c) between the jaws of 70 mm. First, a preload of 20 kN was applied to the specimen to remove any slack in the system; this was applied at a displacement rate of 0.005 m/min. Then, an initial strain rate of 0.00007 s^{-1} was applied until a total strain of 1% was reached, and then the strain rate of was increased to 0.00025 s^{-1} gradually, over a 5 minute period, to avoid any sudden changes in the stress-strain response. This strain rate was maintained until failure of the rebar.

Figure 4 – Complete tensile testing setup on the Instron 5584, with the Instron EX2620-601 extensometer.

4.0 Material characterization

One of the key aims of this work was to study not only the mechanical characteristics of duplex stainless steel reinforcement following fire exposure but also the key metallurgical phenomena that occur, in order to develop a full understanding of the behaviour. As with all duplex stainless steel alloys, prominent austenite and ferrite grains are present. In this work, material characterization was carried out to determine if there is a change between the balance in the austenite and ferrite grains following elevated temperature exposure and to understand the consequent change in microstructure. This was done using two methods (i) an initial inspection was conducted through X-ray diffraction (XRD), for phase identification and monitoring of phase changes, and (ii) through microscopic imagery to obtain a visual inspection of the size, shape and dispersion of the grains.

4.1 XRD examination

The diffractograms obtained from the XRD investigation are given in Figs. 5 and 6, and indicate the presence of the phase (intensity) against the angle of discovery (2theta). Fig. 5 presents the data for hot-rolled grade 1.4362 reinforcing bars that were heated to various temperatures as indicated and then cooled either (a) by quenching in cold water, (b) naturally, in air, or (c) slowly, in the furnace at a controlled rate of 1°C/min. Fig. 6 presents the corresponding images for the cold-rolled rebars. The position of both the austenite (solid dot) and ferrite (empty dot) peaks are labelled in the images along the x-axis. Notably, for 2theta, only between 40°-90° is presented as this is the range prone to significant change.

There is no significant change of phase visible for specimens that were cooled at different rates. The diffractograms for both the hot- and cold-rolled samples remain almost identical, with phase peaks at the same location. Through further analysis using the DIFFRAC.EVA phase identification software [21], the ratio of austenite to ferrite was found to be 1:3, or 25% austenite and 75% ferrite, on average, for both the virgin cold-rolled and hot-rolled samples. The 1:3 ratio was consistent for the cold-rolled samples, with the exception of the air-cooled samples at 700°C, which presented an increase to 35% austenite and 65% ferrite retention, which can also be observed in Fig. 6(b). For the hot-rolled samples, the austenite-ferrite ratio was significantly less stable, with the samples that were heated to 500°C and 800-900°C before being quenched or slow-cooled presenting a change of austenite between 35-40% and a retention of ferrite between 60-65%; all of the air-cooled samples remained stable. Austenite is more stable than ferrite at higher temperatures, for the quenched and slow-cooled samples, the conditions for the ferrite nucleation are not met, resulting in a decline in the ferrite content and a rise in the austenite grains.

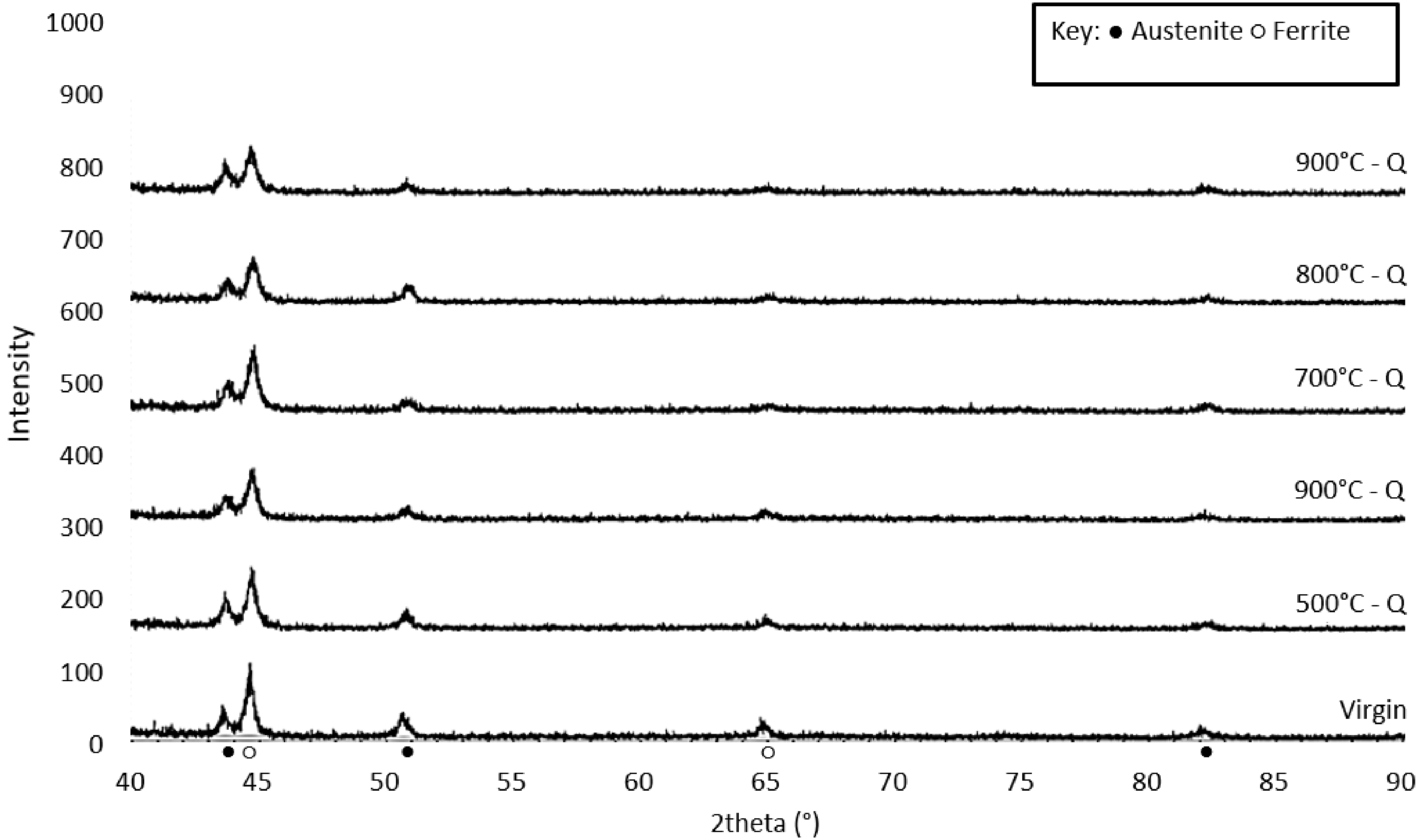
Key: ● Austenite ○ Ferrite
Intensity
2theta (°)
900°C - Q
800°C - Q
700°C - Q
900°C - Q
500°C - Q
Virgin
0
100
200
300
400
500
600
700
800
900
1000
40
45
50
55
60
65
70
75
80
85
90

(a)

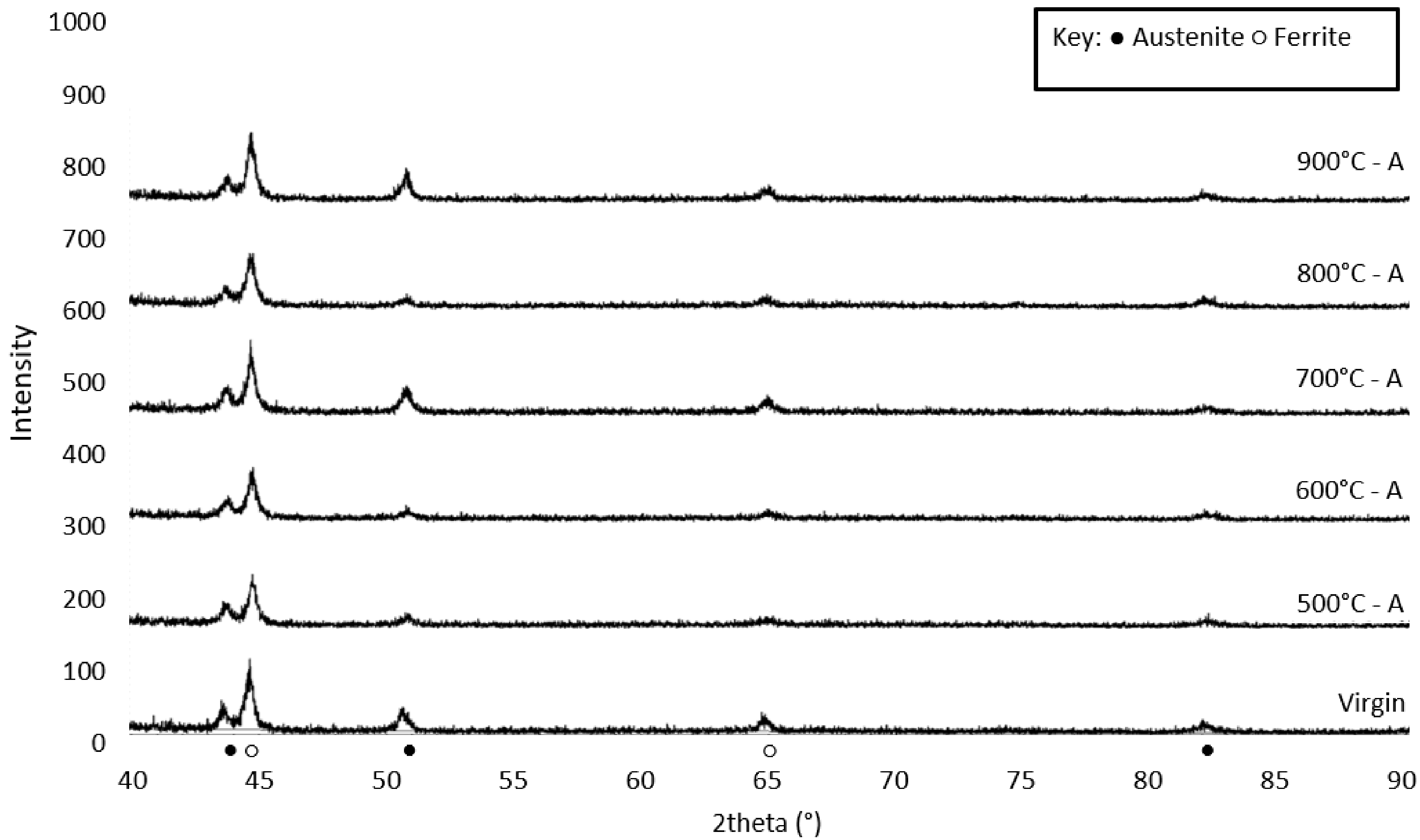
Key: ● Austenite ○ Ferrite
1000
900
800
700
600
500
400
300
200
100
0
Intensity
900°C - A
800°C - A
700°C - A
600°C - A
500°C - A
Virgin
40
45
50
55
60
65
70
75
80
85
90
2theta (°)

(b)

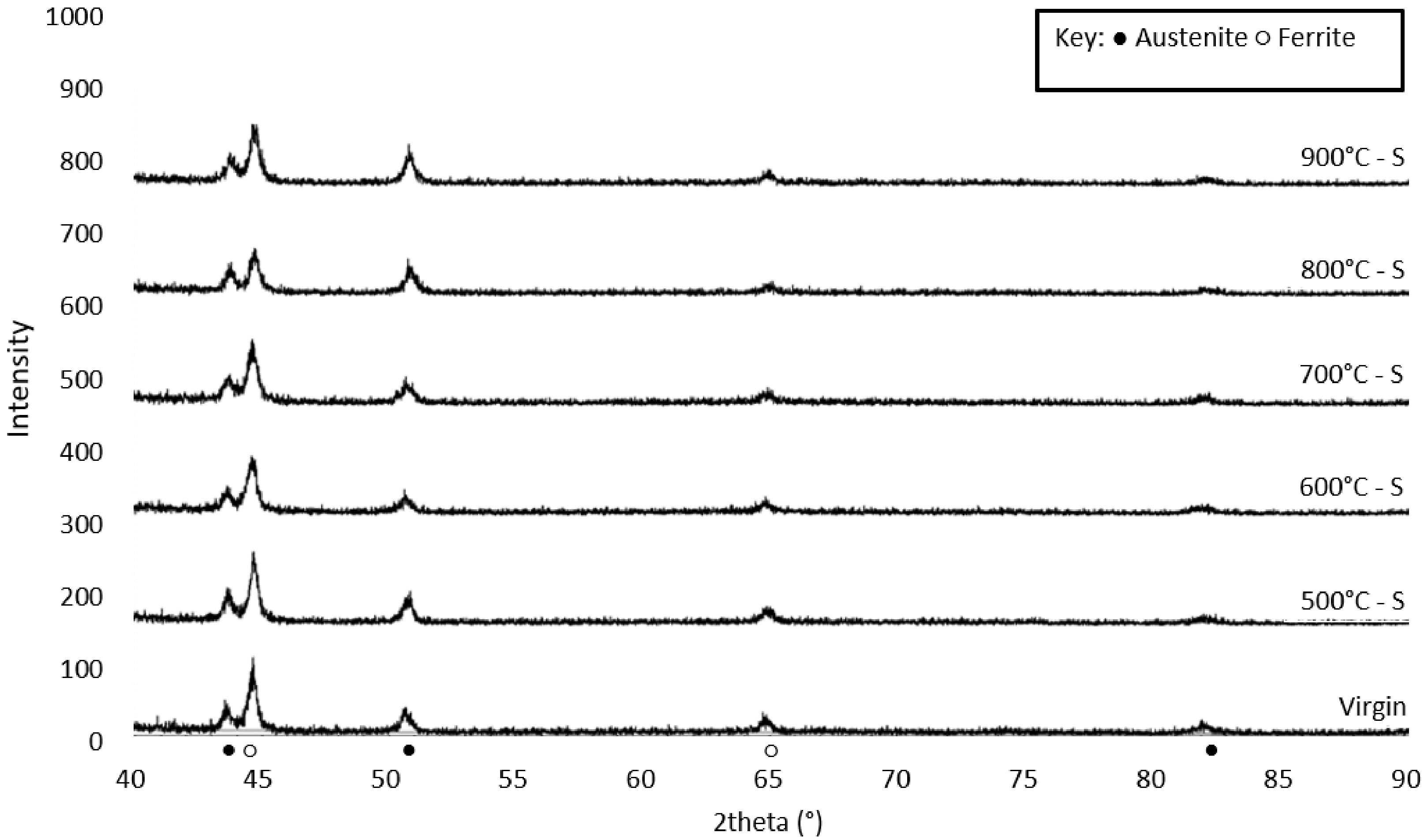

(c)

Figure 5 Diffractograms for grade 1.4362 hot-rolled reinforcing bar that were heated to various temperatures as indicated and then cooled (a) quickly, by quenching in cold water, (b) naturally, in air, and (c) slowly, in the furnace.

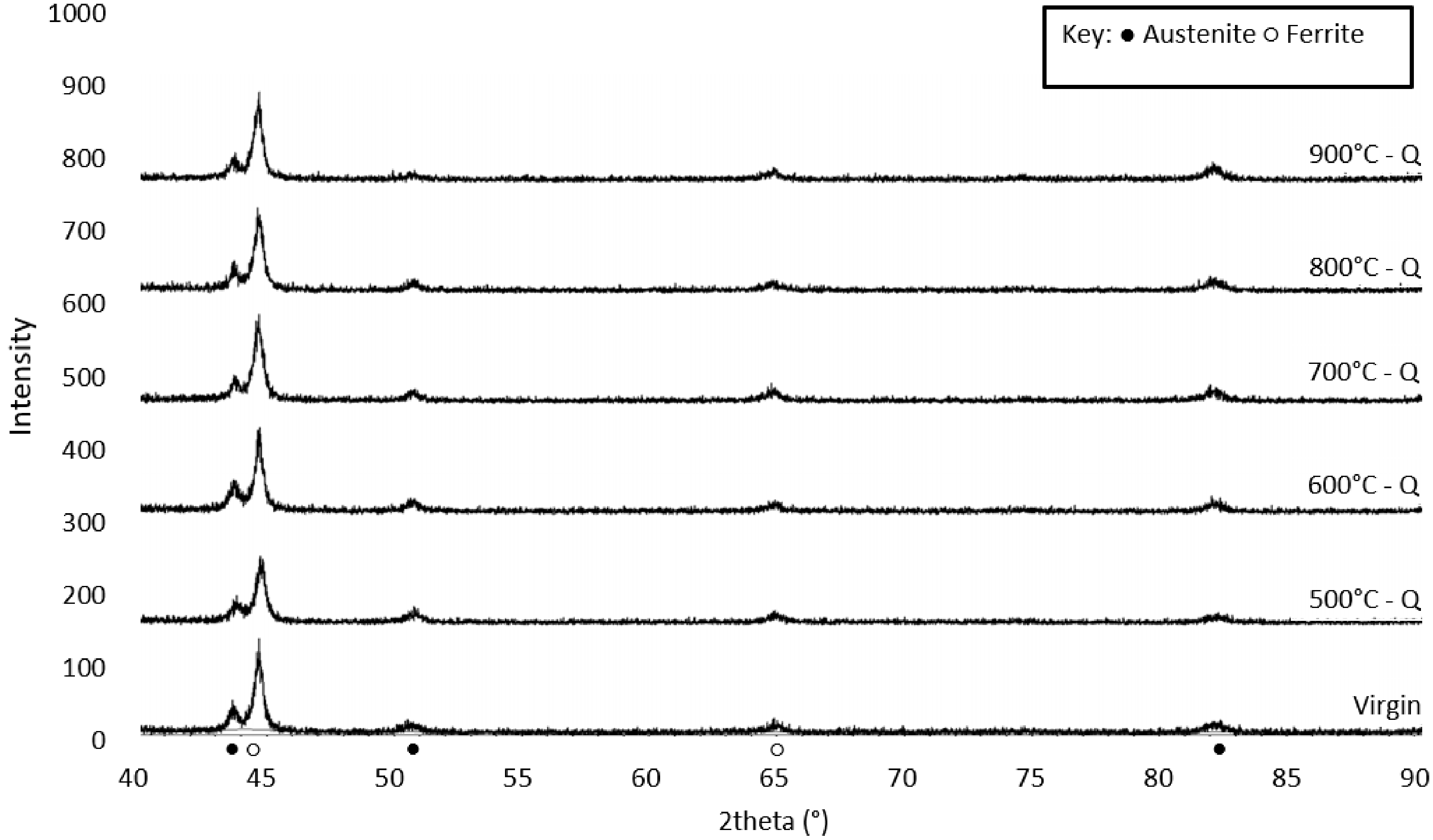
Key: ● Austenite ○ Ferrite
1000
900
800
700
600
500
400
300
200
100
0
Intensity
900°C - Q
800°C - Q
700°C - Q
600°C - Q
500°C - Q
Virgin
40
45
50
55
60
65
70
75
80
85
90
2theta (°)

(a)

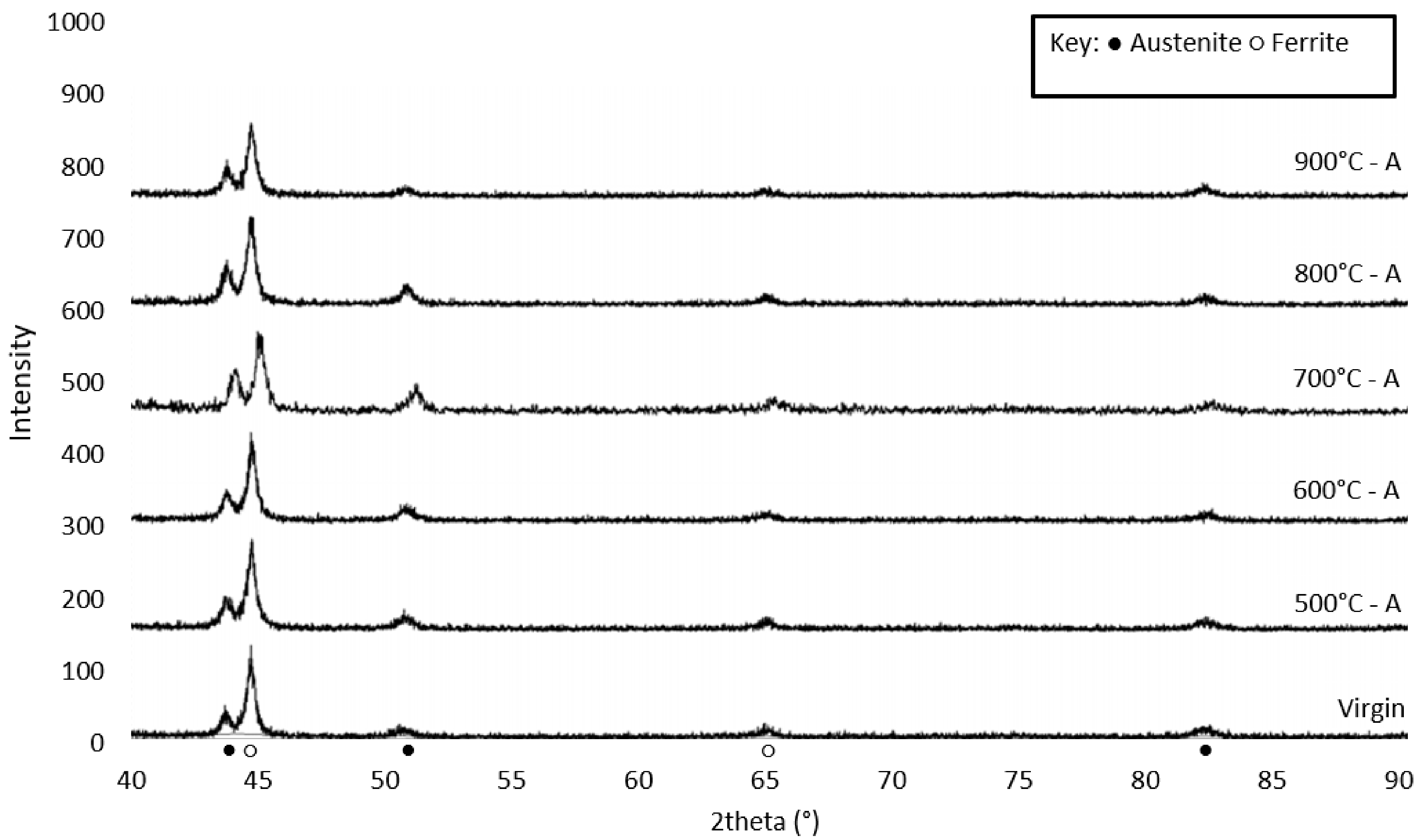

Key: ● Austenite ○ Ferrite
900°C - A
800°C - A
700°C - A
600°C - A
500°C - A
Virgin
Intensity
2theta (°)
0
100
200
300
400
500
600
700
800
900
1000
40
45
50
55
60
65
70
75
80
85
90

(b)

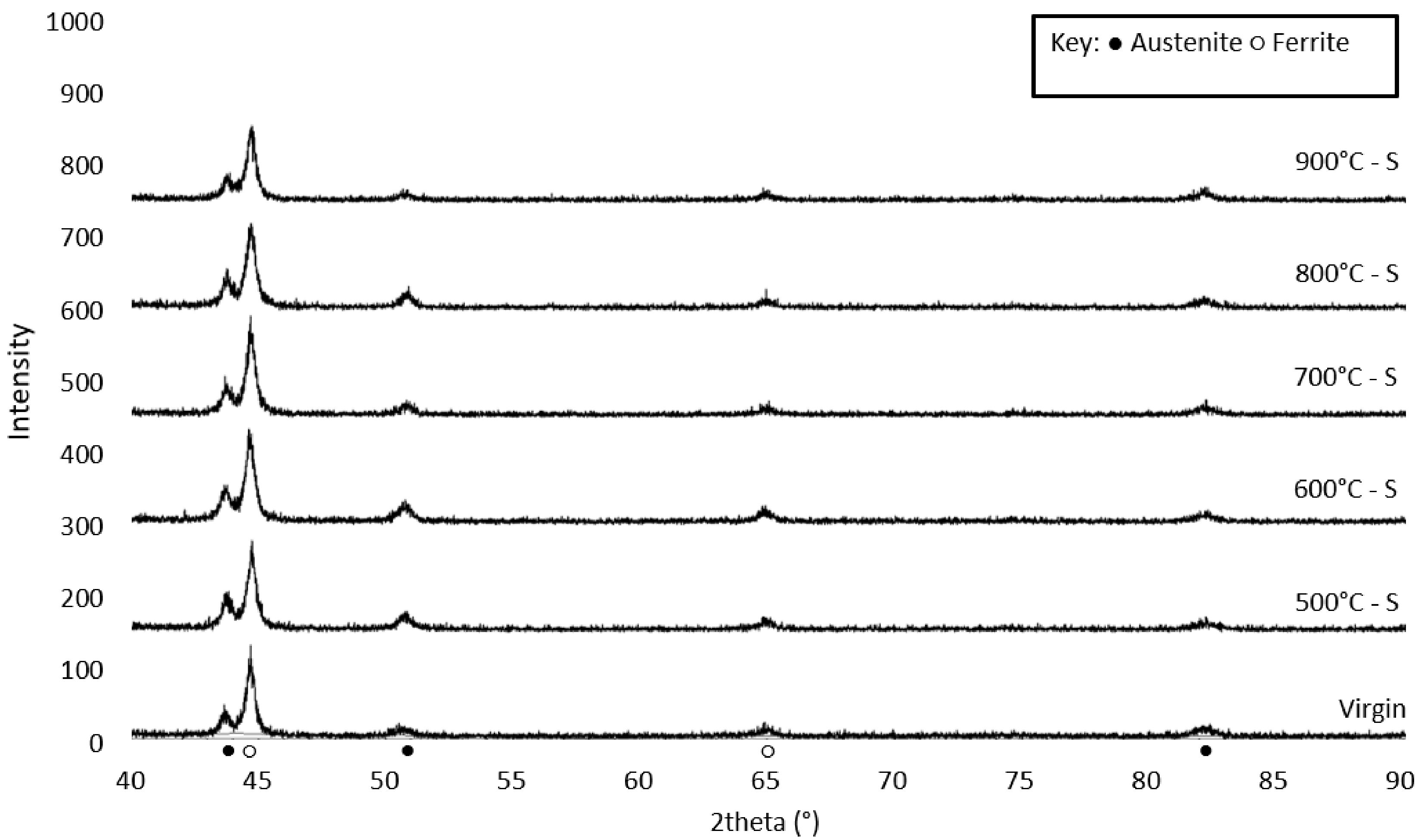

(c)

Figure 6 Diffractograms for grade 1.4362 cold-rolled reinforcing bar that were heated to the various temperatures as indicated and then cooled (a) quickly, by quenching in cold water, (b) naturally, in air, and (c) slowly, in the furnace.

4.2 Microscopic investigation

Microscopic imagery enables a visual inspection of the size, shape and dispersion of the grains in a metallic material. To study the change in grains for grade 1.4363 duplex stainless steel reinforcement, the complete imagery is presented in Fig. 7, for (a) the hot-rolled rebars in their virgin (i.e. unheated) state, (b) the equivalent images for the cold-rolled virgin materials, (c) the cold-rolled rebars exposed to 700°C and subsequently quenched in water to cool rapidly, (d) the cold-rolled bars exposed to 700°C and subsequently air-cooled, (e) the cold-rolled reinforcing bar exposed to 700°C and subsequently slow-cooled, and (f) the cold-rolled rebars exposed to 700°C and subsequently slow-cooled, magnified to enable a closer inspection. The bars that were heated to 700°C are selected here for illustrative purposes and because this was the lowest level of temperature exposure at which the bars retained comparable mechanical properties to their virgin values, in the mechanical testing. It should be noted that at this stage, due to the duplex nature of the alloy, both austenite and ferrite are present, and these are identified as δ-ferrite which are darker grains in the images and γ-austenite which are the lighter grains.

For the the virgin hot-rolled sample as shown in Fig. 7(a), several small grain clusters can be found, and these smaller grains are formed from larger recrystalising during the hot-rolling process. The small grains act as the primary strengthening mechanism for hot-rolled reinforcing bars. This is explained by the Hall-Petch relationship which indicates that the smaller the grain size, the higher the material strength [22]. For the cold-rolled virgin sample as shown in Fig. 7(b), the primary strengthening mechanism is the formation of α′-martensite in the γ-austenite grains during the cold-rolling process as a response to the stresses induced by the manufacturing process pushing the material to recrystallise. Deformation in the δ-ferrite grains are minimal as the γ-austenite is more ductile and prone to change, and thus the plastic deformation defaults to the γ-austenite grains. The presence of α′-martensite can be identified through visual grain deformation, as highlighted in Fig. 7(b).

Following exposure to 700°C and subsequent cooling, all three cooling methods as shown in Fig. 7(c-e) present more visible γ-austenite and α′-martensite grains. After exposure to 700°C and subsequent cooling there is good retention of the mechanical properties (i.e. $f_{0.2p}$, f_u, ε_u and ε_f) due to the samples not being exposed to the active recrystallisation temperature of 727°C, after this point, the α′-martensite grains would see active reversion to γ-austenite, resulting in an increase in ductility paired with a loss of strength. For the slow-cooled sample, almost identical mechanical strength (f_u and $f_{0.2p}$) values are retained but, upon close inspection of Fig. 7(f), it is clear that the δ-ferrite grain boundary has undergone change. The grain boundary has a development of nitride precipitation phase present; chromium alloys such as stainless steels are prone to the formation of the σ phase once they are exposed to temperatures in excess of 550°C [23] and then cooled slowly. This is important because the σ-phase compromises the corrosion resistance of the alloy.

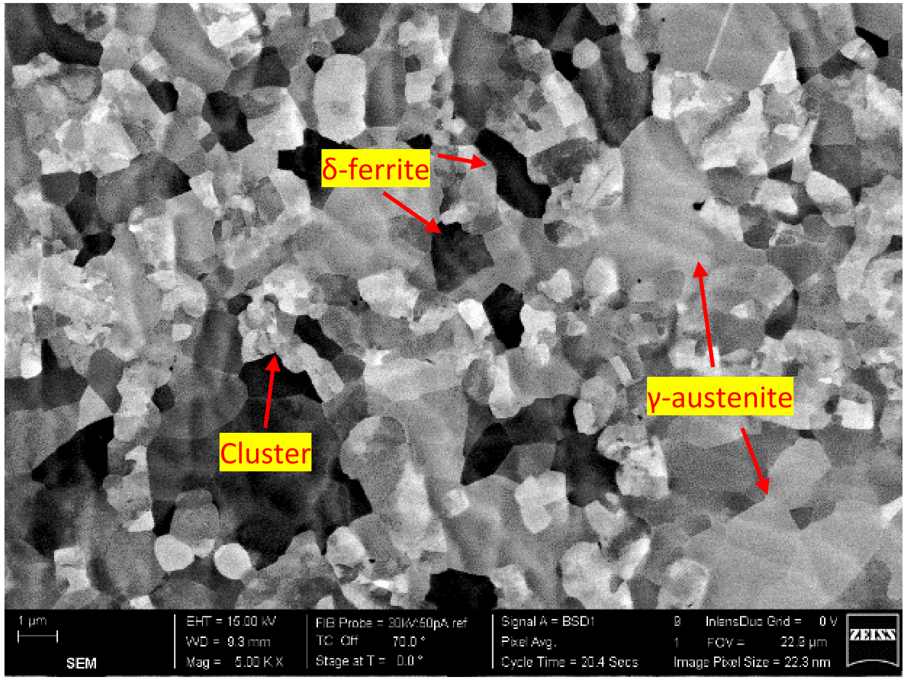
δ-ferrite
Cluster
γ-austenite
1 µm
SEM
EHT = 15.00 kV
WD = 9.3 mm
Mag = 5.00 K X
Signal A = BSD1
Pixel Avg.
Cycle Time = 20.4 Secs
Image Pixel Size = 22.3 nm
ZEISS

(a)

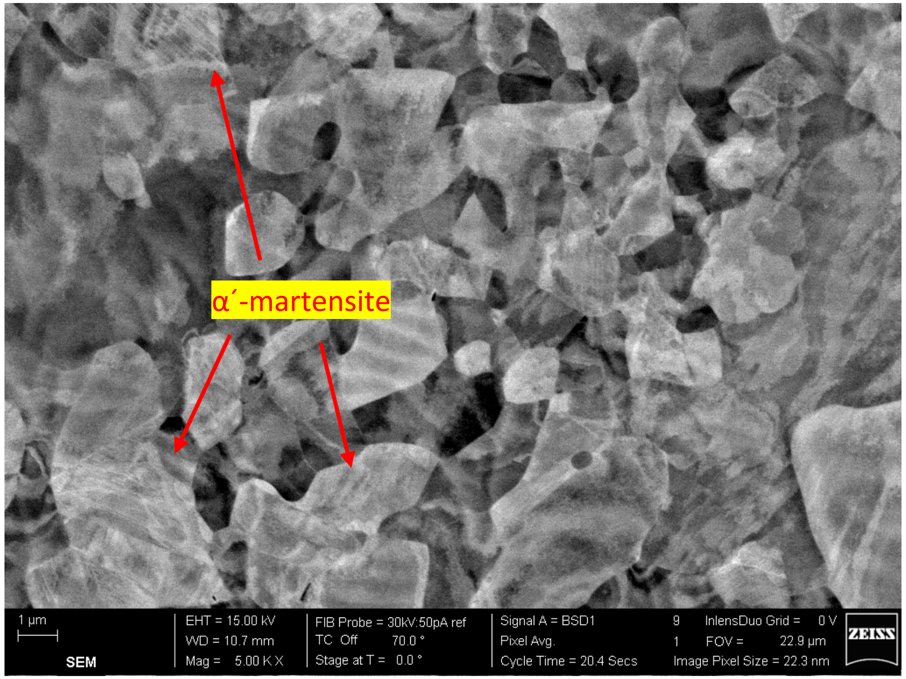
α´-martensite
1 µm
SEM
EHT = 15.00 kV
WD = 10.7 mm
Mag = 5.00 K X
FIB Probe = 30kV:50pA ref
TC Off 70.0 °
Stage at T = 0.0 °
Signal A = BSD1
Pixel Avg.
Cycle Time = 20.4 Secs
InlensDuo Grid = 0 V
FOV = 22.9 µm
Image Pixel Size = 22.3 nm
ZEISS

(b)

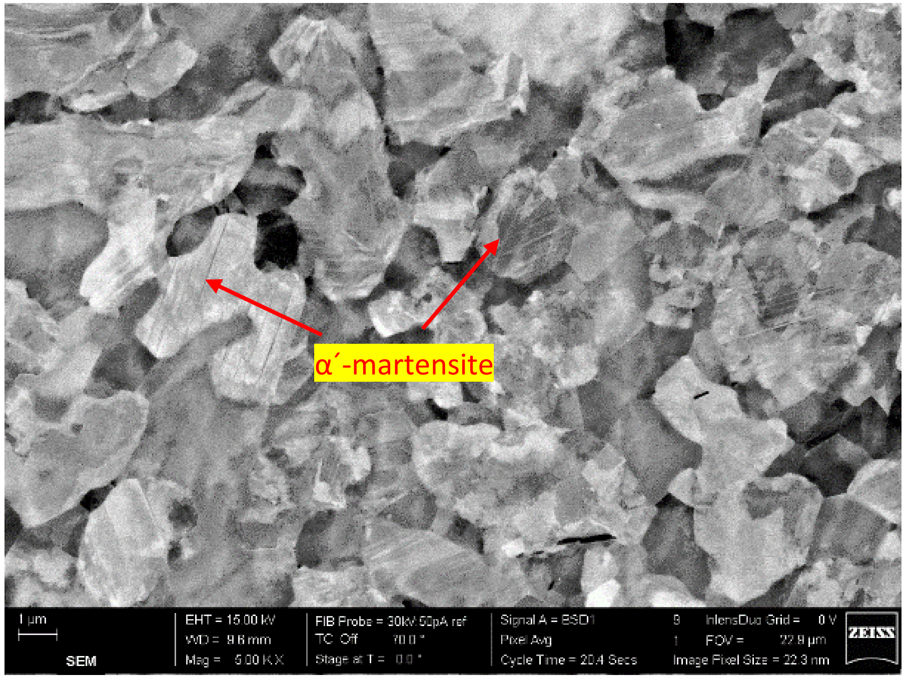
α´-martensite
1 µm
SEM
EHT = 15.00 kV
WD = 9.8 mm
Mag = 5.00 K X
Signal A = BSD1
Pixel Avg.
Cycle Time = 20.4 Secs
FOV = 22.9 µm
Image Pixel Size = 22.3 nm
ZEISS

(c)

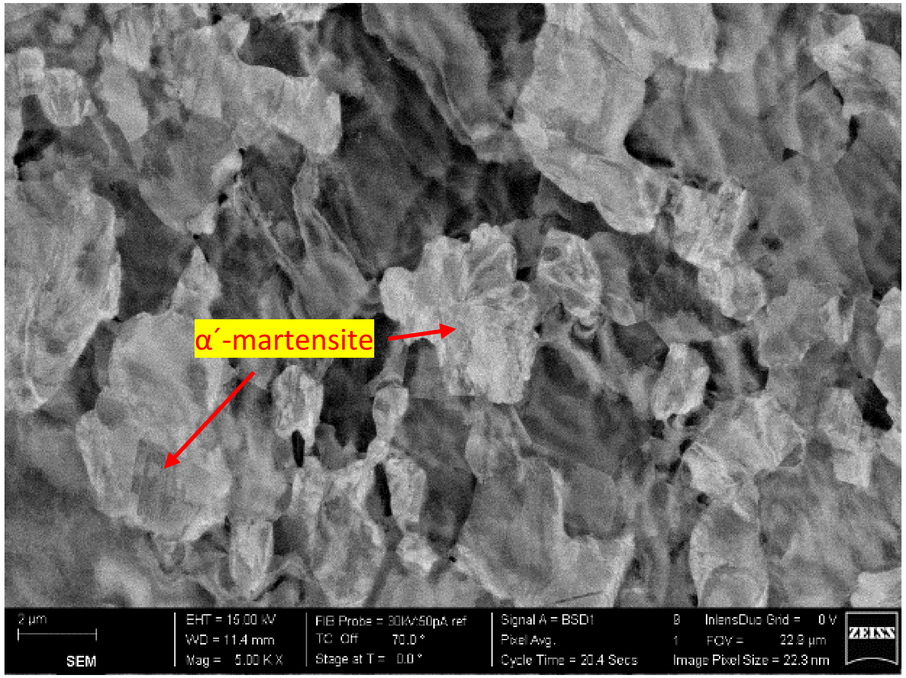
α´-martensite
2 µm
SEM
EHT = 15.00 kV
WD = 11.4 mm
Mag = 5.00 K X
Signal A = BSD1
Pixel Avg.
Cycle Time = 20.4 Secs
FOV = 22.9 µm
Image Pixel Size = 22.3 nm
ZEISS

(d)

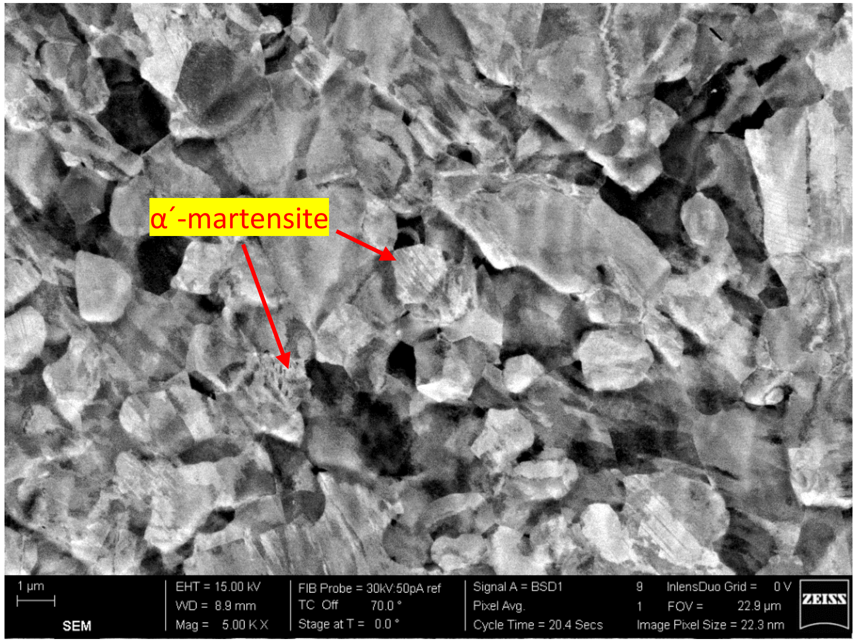

(e)

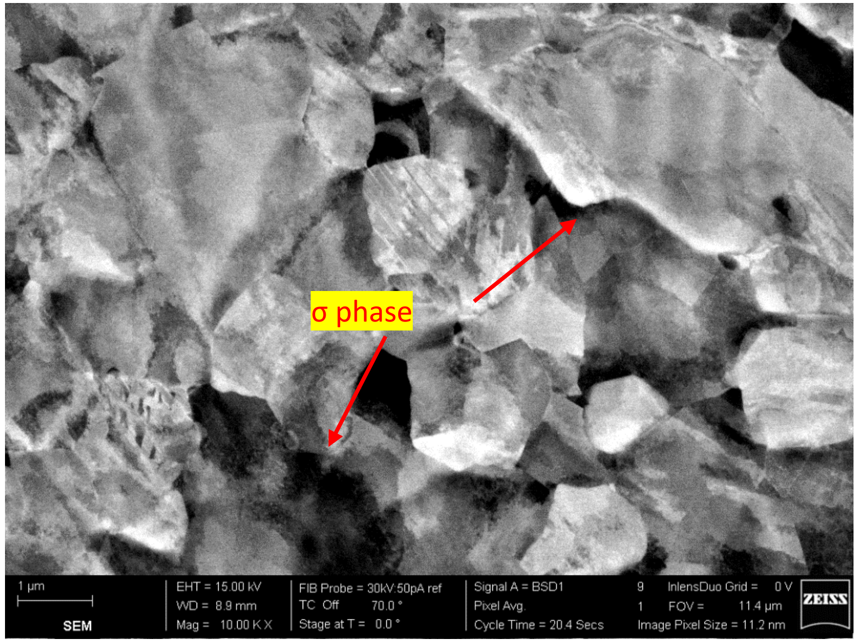

(f)

Figure 7 The grain imagery for grade 1.4362 reinforcing bar including (a) the hot-rolled virgin sample, (b) the cold-rolled virgin sample, (c) the cold-rolled bar exposed to 700°C and subsequently quenched, (d) the cold-rolled bar exposed to 700°C and subsequently air-cooled, (e) the bar exposed to 700°C and subsequently slow-cooled, the bar exposed to 700°C and subsequently slow-cooled further magnified.

5.0 Mechanical test results

A total of 30 tensile tests were conducted on both hot-rolled and cold-rolled specimens following exposure to temperatures of 500-900°C before cooling, with three repetitions carried out for each rebar type at every temperature point. The post-fire residual mechanical properties are presented in Table 4. The values presented include the 0.2% proof stress $f_{0.2p}$, the tensile strength f_u, the percentage total elongation at the maximum force ε_u and the total strain at failure ε_f. A reference system is adopted to name each specimen: the first term is the target exposure temperature (i.e. 500°C, 600°C, 700°C, 800°C or 900°C) and the second parameter is the method of cooling, where Q is for quenched in water, A for air-cooled and S for slow-cooled.

Table 4 – Post fire properties of hot-rolled and cold-rolled duplex grade EN 1.4362 stainless steel

	Hot-rolled				Cold-rolled			
Specimen	$f_{0.2p}$ (N/mm^2)	f_u (N/mm^2)	ε_u (%)	ε_f (%)	$f_{0.2p}$ (N/mm^2)	f_u (N/mm^2)	ε_u (%)	ε_f (%)
Virgin	615.7	803.0	16.0	21.7	836.8	941.5	1.5	19.7
500°C-Q	798.9	848.5	13.5	18.8	924.2	976.6	6.1	22.1
600°C-Q	688.8	803.4	15.6	20.9	848.2	945.8	7.2	18.9
700°C-Q	583.2	785.8	17.4	23.8	735.5	886.9	7.4	22.8
800°C-Q	531.1	774.2	18.4	24.2	529.5	792.9	48.8	59.3
900°C-Q	435.0	713.8	26.5	32.9	429.5	708.0	38.5	59.4
500°C-A	807.4	853.3	18.2	24.5	938.5	1003.3	4.8	19.5
600°C-A	737.5	821.5	16.2	21.5	913.4	981.2	6.1	19.6
700°C-A	625.3	809.2	17.0	22.1	785.4	915.0	7.0	19.4
800°C-A	582.6	793.5	19.9	26.1	605.6	798.6	49.7	59.0
900°C-A	467.4	730.5	26.9	34.1	443.9	731.0	34.4	55.4
500°C-S	828.7	864.5	15.0	20.5	976.1	1006.2	3.7	23.8
600°C-S	757.9	856.9	16.1	21.6	950.2	1004.1	7.4	19.4
700°C-S	683.5	851.5	17.7	23.7	849.0	947.9	7.1	19.7
800°C-S	644.8	821.8	18.4	23.8	636.4	816.1	45.9	56.7
900°C-S	505.4	762.7	24.2	29.9	485.5	760.4	32.4	57.1

5.1 Hot-rolled grade 1.4362 duplex stainless steel rebars

For the hot-rolled specimens, in addition to the data presented in Table 4, the full stress-strain responses are presented in Fig. 8 for (a) the samples quenched in water, (b) the air-cooled samples and (c) the slow-cooled samples. The first observation is that for all three cooling methods, there is a change in shape of the residual stress-strain response between the bars that were heated to 500°C and those that were exposed to higher temperatures, before cooling. There is a distinct yield point visible for all of the bars that were heated to 500°C (and 600°C for the air-cooled specimens only), which was not present for the virgin samples, or those that were heated to higher temperatures. This yield point was followed by a sudden increase in strength. This is an unusual phenomenon for stainless steel material and it is attributed to the nature of the duplex grain boundary. The separate austenite and ferrite grains undergo localised changes in relation to individual mechanical properties, causing a transformation in the grain boundary area [24].

In addition, for the bars that were exposed to 500°C, all three cooling methods responded with a significant increase in $f_{0.2p}$, from 615.7 N/mm^2 for the virgin sample (i.e. room temperature, before exposure to elevated temperature) to 798.9 N/mm^2 for the quenched, 807.4 N/mm^2 for the air-cooled and 828.7 N/mm^2 for the slow-cooled specimens. This represents an increase in the residual 0.2% proof strength of between 30-35% following exposure to 500°C and then subsequent cooling. The increase was greatest for the slowest cooled specimens as the slow-cooled specimens allow for greater setting and definition of the grain, leading to a more stable microstructure following fire exposure. Moreover, it is noteworthy that 500°C is the annealing point for this material [5], and therefore changes in properties are to be expected. The residual value for the total strength f_u also increased following exposure to 500°C and cooling, although not to the same extent as $f_{0.2p}$. The increase in the residual f_u value was between 6-8%, with the slowest cooled specimens again showing the greatest increase of the three cooling rates examined. This disproportionate change in the residual values of $f_{0.2p}$ and f_u results in the specimens cooled by all three cooling methods failing the $f_u/f_{0.2p}$ stress ratio requirement as outlined in BS 6744 [18] and Annex C of Eurocode 2 Part 1-1 [25]. This stipulates that in order to meet ductility Class B, $f_u/f_{0.2p}$ should be equal to at least 1.08. In this study, the stress ratio for the post-fire properties of the quenched samples has a value of 1.062, the air-cooled sample is 1.056 and the slow-cooled sample is 1.043.

The strain response shows a similar level of reduction for the residual values of both the ultimate strain ε_u and the total strain at failure ε_f, although there was significant variation in the level of reduction depending on the cooling rate. The samples that were quenched in water, and therefore cooled the quickest, had a residual value for ε_f which is 13% less than the corresponding virgin specimen. On the other hand, the air-cooled bars showed an increase in residual ε_f of 13% and the slow-cooled samples had a reduction in ε_f compared with the corresponding virgin sample of 6%. It is noteworthy that the specimens that were cooled the quickest and the slowest of the three scenarios both exhibited a reduction in ε_f compared to their corresponding virgin values, whereas the specimens that were heated at an intermediary rate had an increase in residual ε_f. This is most likely owing to the metallurgical changes that take place. As previously discussed, the grain boundary between the austenitic and ferritic grains is very unstable and can lead to unpredictable results for strains.

After exposure to 600°C there was a lower increase in the residual value of $f_{0.2p}$ compared to f_u allowing for the required stress ratio of at least 1.08 to be achieved across all three cooling methods. A trend is established for the residual strength, with the quenched samples showing the lowest increase of the three cooling rates examined at 12% for $f_{0.2p}$ and just over 1% for the f_u. The air-cooled samples had an intermediary increase of 20% for $f_{0.2p}$ and 2% for f_u. The slow cooled samples had the greatest rise relative to the virgin sample of 23% for $f_{0.2p}$ and 7% for f_u. The strain response demonstrated minimal change across all three cooling methods, remaining at just over 1% for both ε_u and ε_f for the air-cooled and slow-cooled methods, whereas the quenched had a 2% reduction in ε_f and 4% at ε_u.

After exposure at 700°C and subsequent cooling, the variations in the strength response between the cooling methods becomes more noticeable. Compared with the corresponding virgin samples, for the quenched samples, there was a reduction in residual $f_{0.2p}$ and f_u of 5% and 2%, respectively. For the air-cooled rebars, there was an increase in residual strength compared to the virgin values of 2% for $f_{0.2p}$ and 1% for f_u. The slow-cooled rebars showed the greatest residual increases of 11% for $f_{0.2p}$ and 6% for f_u. For the strain response there was a minor increase across all three cooling methods, but with no notable pattern between the different cooling regimes. Overall, ε_u increased by between 6-11% compared with the virgin values following heating to 700°C and subsequent cooling, whilst the corresponding range for ε_f was between 2-10%.

A consistent trend in these observations is also shown for the bars that were exposed to temperatures of 800°C and then cooled. For those that were cooled quickly, by quenching in cold water, the specimens showed a large decrease of 14% in the residual value of $f_{0.2p}$ compared with the corresponding virgin values. There was also a reduction in residual $f_{0.2p}$ of 5% for the air-cooled samples compared with the virgin values. Conversely, for the slowest-cooled specimens, there was an increase in residual $f_{0.2p}$ of 5% compared with the virgin samples. The tensile strength f_u followed the same trend but the cooling rate had a negligible influence on the post-fire values. There was a reduction of 4% compared with the virgin f_u value for the quenched samples, a decrease of 1% for the air-cooled bars and an increase of 2% for the slow-cooled specimens. On the other hand, the strain response had an increase of 15-24% for ε_u and 10-20% for ε_f, compared with the corresponding virgin values, with no clear pattern for the different cooling rates.

After exposure to this highest temperature examined in this programme, 900°C, the previously-discussed trends of a reduction of residual strength and an increase in ductility for all three cooling methods are more significant. The loss of strength across the various cooling methods was most prominent for the quenched samples, whilst the slow-cooled rebars retained the greatest proportion of their original strength. A reduction of 18-29% was found in the $f_{0.2p}$ whereas the f_u reduced by between 5-11%. Additionally, with the exception of the slow-cooled samples, which retained $f_{0.2p}$ values of 505.4 N/mm^2, the air-cooled and quenched samples failed to meet the technical $f_{0.2p}$ requirement of 480 N/mm^2 set out in BS6744 [18].

A closer inspection of the variations in behaviour between the three different cooling methods is presented in Fig. 9; in this image, the data for hot-rolled grade 1.4362 rebars is presented, for illustration. For all temperature levels, the slow-cooled bars have the highest levels of strength retention overall, followed by the air-cooled bars and then the samples that were quenched. The level of strength loss for the quenched was greatest for those bars that were exposed to relatively higher temperatures. The opposite trend is observed for the air-cooled samples, as those samples that were heated to relatively low levels of elevated temperature experienced a greater relative loss in strength than those that were heated to higher temperatures. This is similar for the slow-cooled samples, which experienced greater changes in the residual strength properties following exposure to relatively low levels of elevated temperature prior to cooling. For the slow cooled samples, at the lower temperature range the most increase was noted against the virgin samples, and for the high temperature range the least loss was noted.

It is more challenging to draw conclusions about the residual ductility and strain behaviour compared with the strength response, as the differences between the three cooling methods were less significant. All of the samples examined in this programme achieved the required strain requirements of at least 5% ε_u and 14% ε_f following exposure to elevated temperature and then cooling, at any rate.

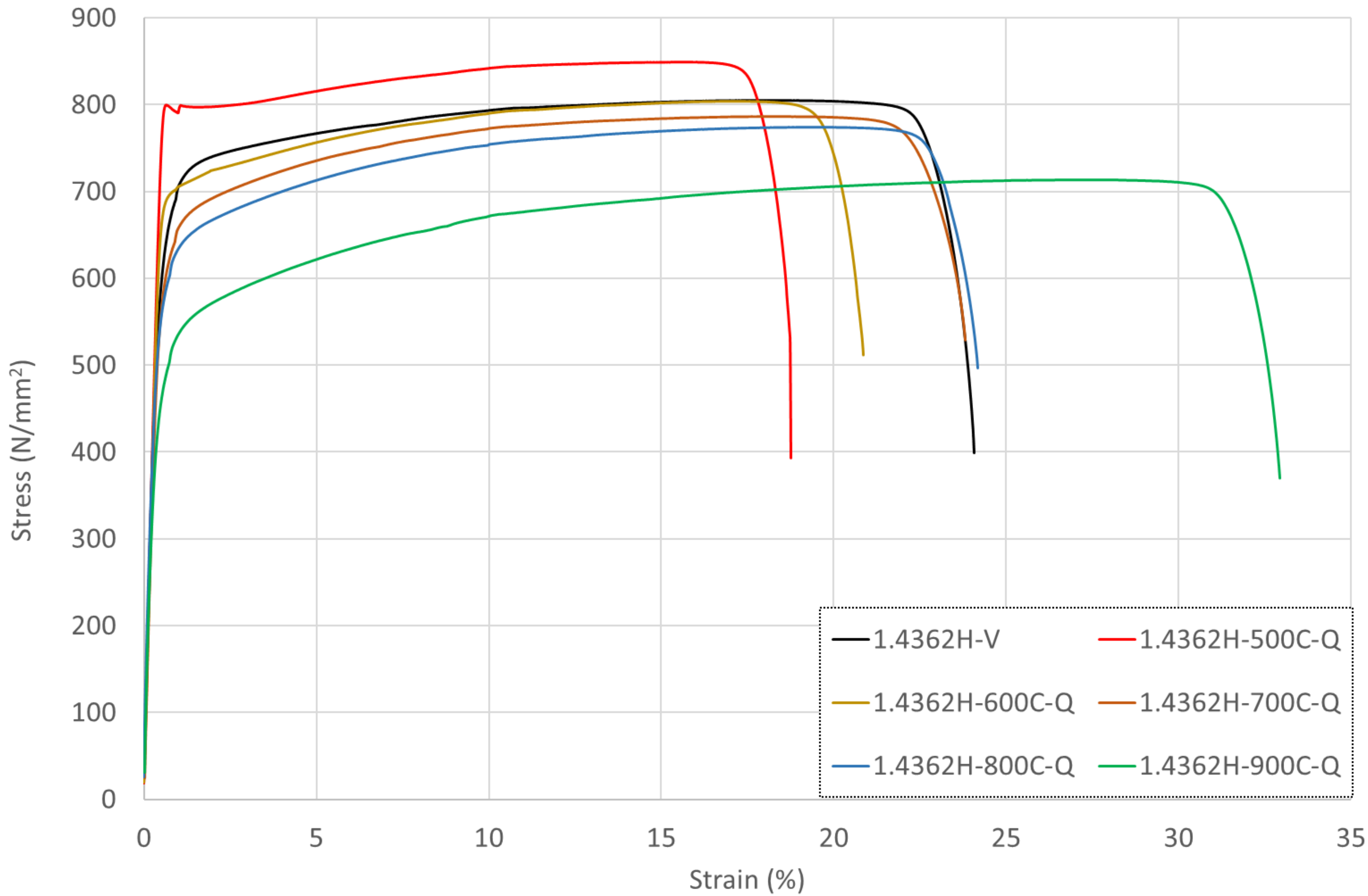

900
800
700
600
500
400
300
200
100
0
Stress (N/mm²)
0
5
10
15
20
25
30
35
Strain (%)
1.4362H-V
1.4362H-500C-Q
1.4362H-600C-Q
1.4362H-700C-Q
1.4362H-800C-Q
1.4362H-900C-Q

(a)

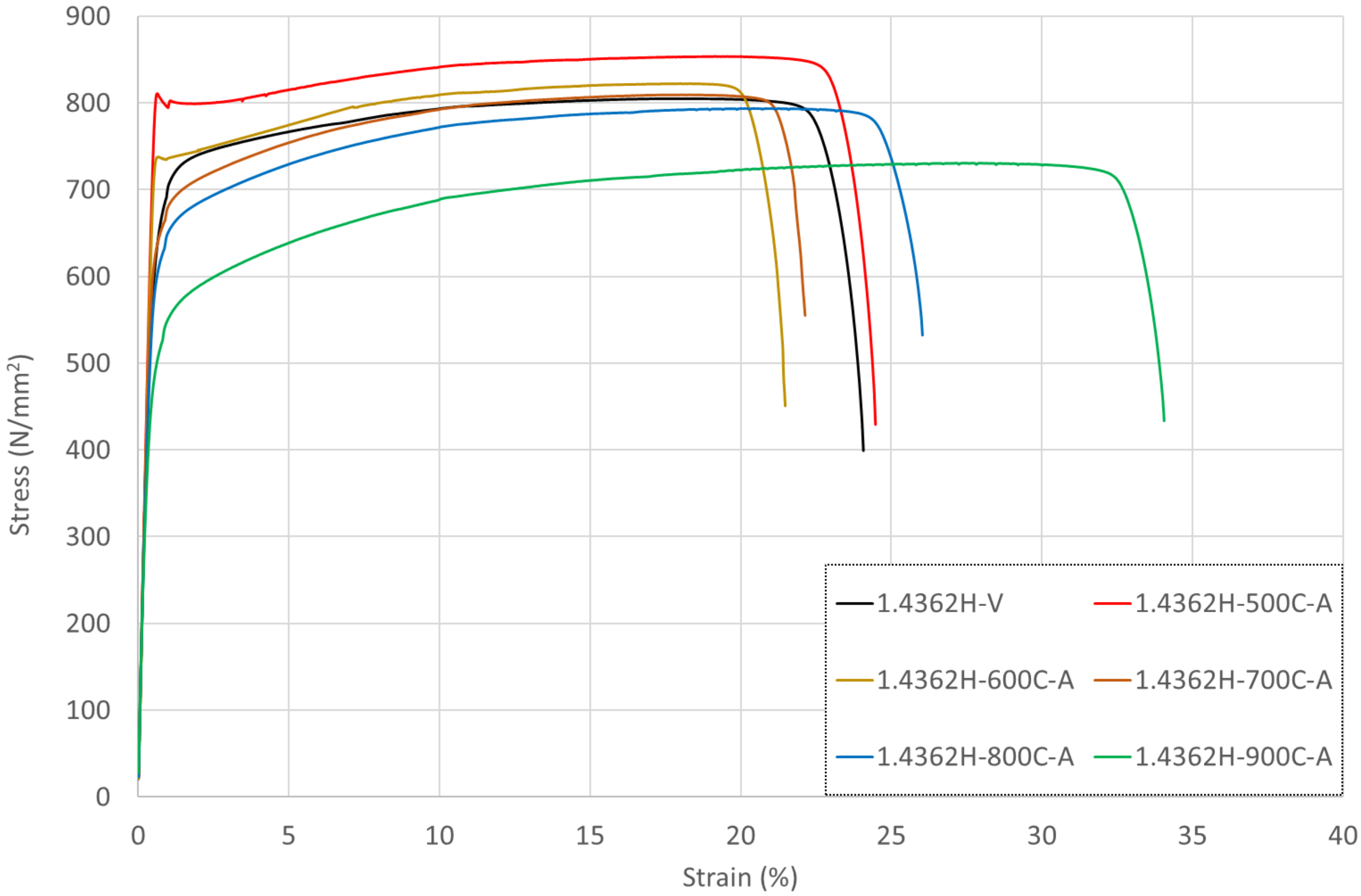

900
800
700
600
500
400
300
200
100
0
Stress (N/mm²)
0
5
10
15
20
25
30
35
40
Strain (%)
1.4362H-V
1.4362H-500C-A
1.4362H-600C-A
1.4362H-700C-A
1.4362H-800C-A
1.4362H-900C-A

(b)

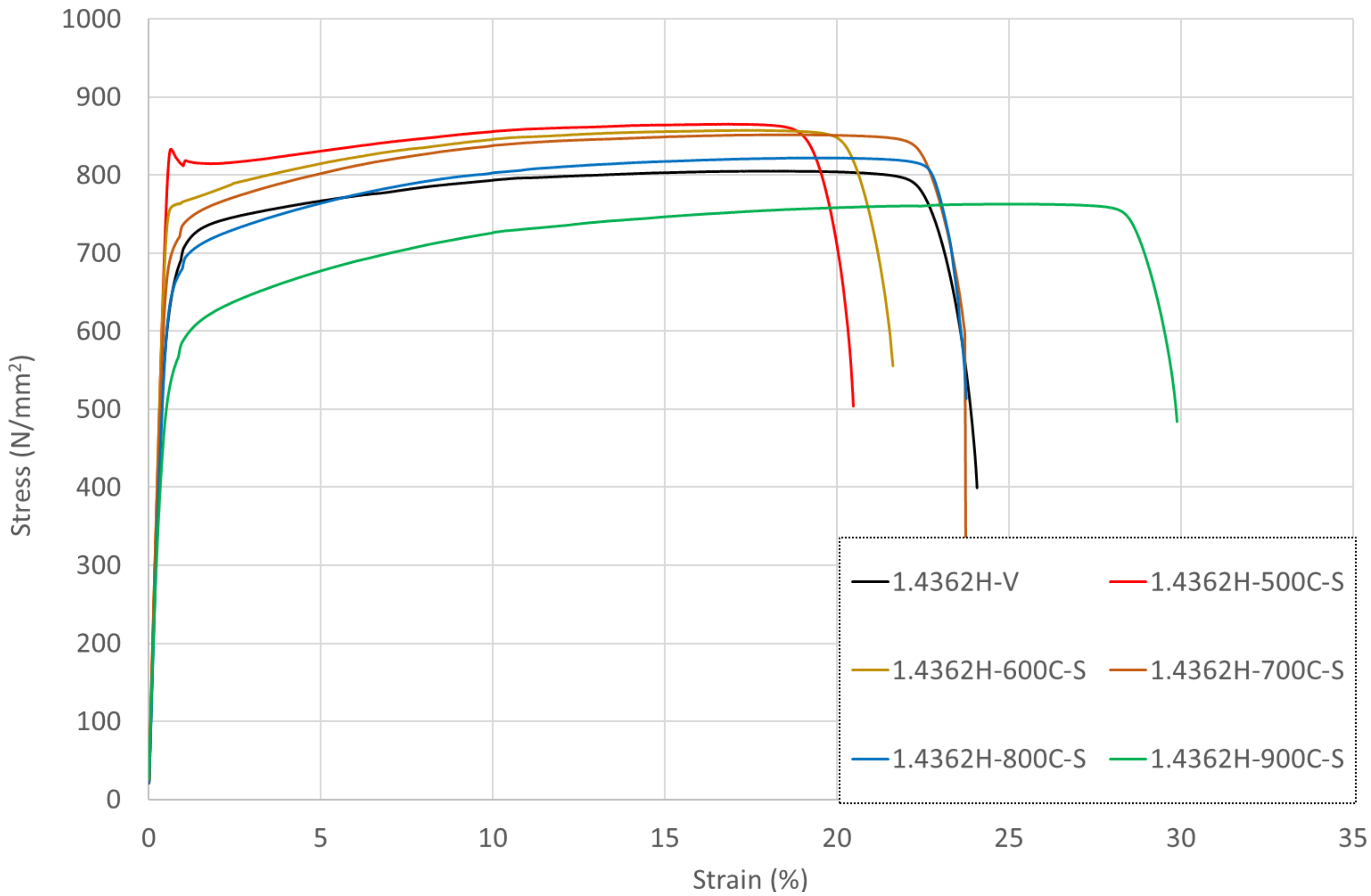

(c)

Figure 8 Stress-strain response for grade 1.4362 hot-rolled duplex stainless steel rebars following exposure to various degrees of elevated temperature and then cooled by (a) quenching in water, (b) naturally, in air and (c) slowly, in the furnace

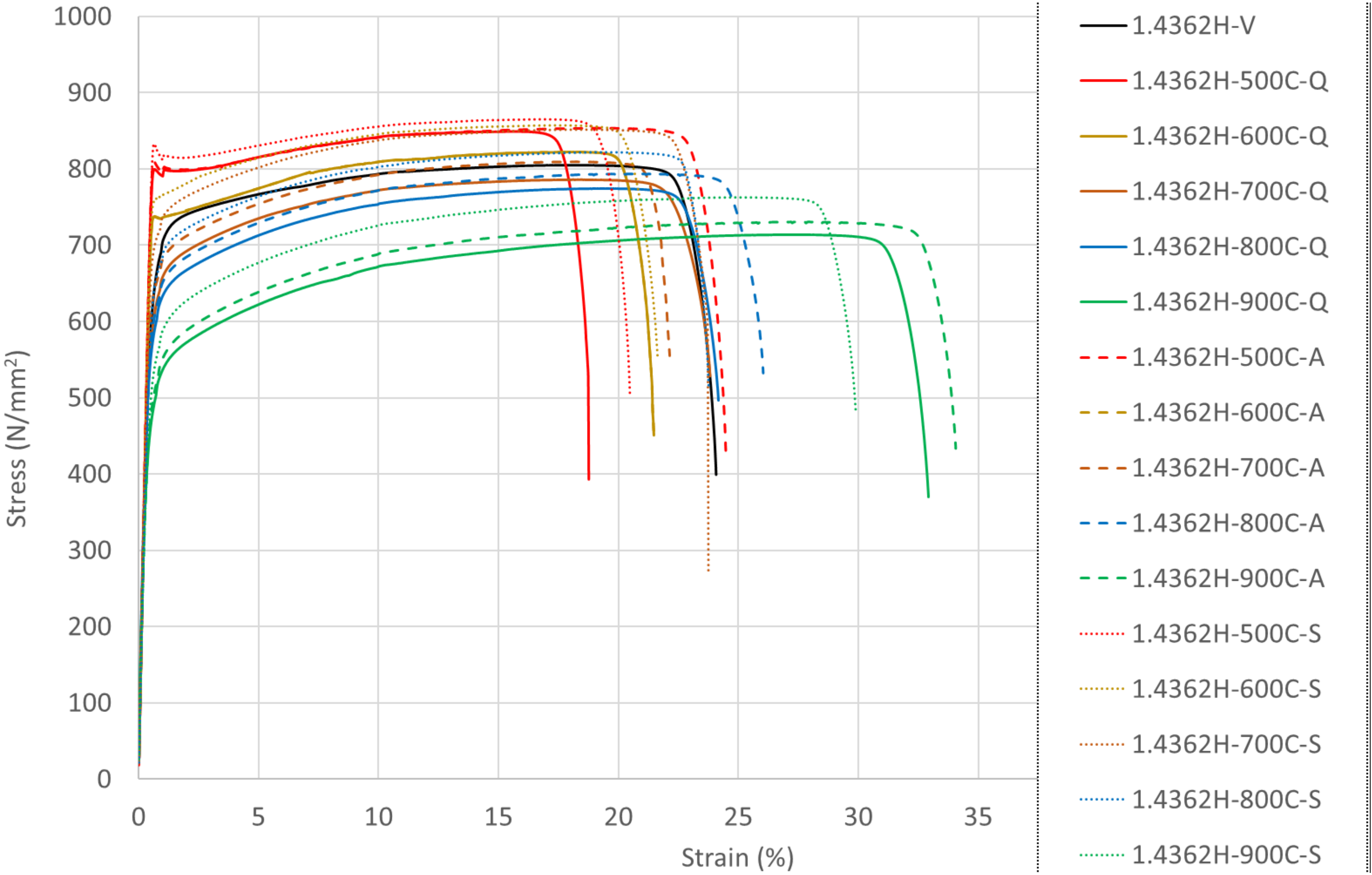

Figure 9 Stress-strain response for grade 1.4362 hot-rolled duplex stainless steel rebars following heating to various temperature before subsequent cooling

5.2 Cold-rolled grade 1.4362 rebar

This section presents and analyses the data from the mechanical tests on cold-rolled grade 1.4362 duplex stainless steel reinforcing bar, making comparisons with the equivalent hot-rolled rebars where appropriate. The numerical data is given in Table 4 and Fig. 10 presents the stress-strain responses for all of the cold-rolled specimens following exposure to elevated temperatures between 500-900°C and subsequent cooling through either (a) quenching, (b) air-cooling or (c) slow-cooling. Before assessing the residual values post-heating, it is noteworthy to observe the significant differences between the virgin sample values for the hot-rolled and cold-rolled rebars. The $f_{0.2p}$ and f_u values were 615.7 N/mm^2 and 803.0 N/mm^2, respectively, for the hot-rolled bars and 836.8 N/mm^2 and 941.5 N/mm^2, respectively, for the cold-rolled rebars in the same grade. Even more notable is the differences in strain values; ε_u was 16% for the hot-rolled rebars and just 1.5% for the cold-rolled bars.

For the post-fire samples, following exposure to either 500°C or 600°C, all of the samples exhibited an increase in strength, both $f_{0.2p}$ and f_u, compared with the unheated virgin samples, regardless of the cooling method. This pattern reversed for the bars that were heated to higher temperatures before cooling, as they lost strength. Considering first the specimens that were heated to 500°C, the bars that were quenched in water had the lowest increase in $f_{0.2p}$, rising to 924.2 N/mm^2, followed by the air-cooled samples which increased to 938.5 N/mm^2 and then the slow-cooled samples which had the greatest increase in residual 0.2% proof strength, changing to 976.1 N/mm^2; these values equate to increases of between 10-17% compared with the virgin values. On the other hand, f_u showed an increase of between 4-7% compared with the virgin values. The residual $f_{0.2p}$ and f_u strength values following exposure to 500°C result in these bars failing to meet the stress ratio criteria of $f_u/f_{0.2p}$ being at least equal to 1.08. The quenched samples had a stress ratio of 1.057, the air-cooled sample was 1.069 and the slow-cooled sample was 1.031.

From the stress-strain responses presented in Fig. 10, the changes in residual strains following exposure to 500°C and then cooling are different to those observed for the hot-rolled bars. For the cold-rolled bars, ε_u changed from 1.5% for the virgin sample to 6.1%, 4.8% and 3.7% for the quenched, air-cooled and slow-cooled samples, respectively. This is because some, and differing, levels of the cold-working in the material was permanently lost following heating. The differences in ε_f following heating and cooling were much more similar to those observed for the hot-rolled bars. This property ε_u changed from 19.7% for the virgin sample to 22.1%, 19.5% and 23.8% for the quenched, air-cooled and slow-cooled samples, respectively.

For the samples exposed to temperatures of 600°C and then subsequently cooled, the response is very similar to that of the 500°C sample set. For $f_{0.2p}$, the quenched samples presented the least variation relative to the virgin specimens, with an increase of 1% from 836.8 N/mm^2 to 848.2 N/mm^2 for $f_{0.2p}$, whereas the air-cooled sample presented a rise of 9% to 913.4 N/mm^2, and the slow-cooled samples rose by 14% to 950.2 N/mm^2. On the other hand, the f_u values also increased by 1%, 4% and 7%, for the quenched, air-cooled and slow-cooled samples, respectively. As the quenched samples reflect the least change from the virgin values, these meet the stress ratio requirement of 1.08 with a ratio of 1.115, whilst the air-cooled and slow-cooled bars fail to meet this requirement with ratios of 1.074 and 1.058, respectively. For the strain response, a more consistent increase between the three cooling methods was observed, with ε_u rising by between 321%-413% overall and ε_f presenting a loss of between 1-4% against the virgin sample. It is clear that for the cold-rolled duplex stainless steel samples, there are different behaviours between the ultimate and failure strains. In cold-rolled rebars, the ultimate strain occurs sooner in the overall stress-strain curve as the material gains more ductility in the elastic region following heating and cooling, as the grains relax. The ferrite grains are more prone to change within this temperature range compared with the austenite grains, and tend to lose any cold-rolling properties. The microstructural features induced through the cold-rolling process begin to dissipate in the ferrite grains following heating, and the stress strain curves begins to change shape to match a more idealized stainless steel curve as shown in Fig. 3, whereas the cold-rolled properties induced into the austenite show little to no difference.

Following exposure to 700°C and subsequent cooling, the residual $f_{0.2p}$ values were dependent on the cooling method. The samples that were cooled quickly by quenching lost some strength, decreasing by 12% to 735.5 N/mm^2 compared with 836.8 N/mm^2 for the virgin samples. Similarly, the air-cooled samples also lost strength recording a residual value for $f_{0.2p}$ of 785.4N/mm^2 (a reduction of 4%). On the other hand, the slow-cooled samples did not change to a great extent and in fact increased by 1% to 849 N/mm^2. In this temperature range, the austinite grains gradually begin to dissipate the cold-worked strength but as the change is very minor, they require rapid cooling to stabilise this change; therefore, a relatively slower cooling rate results in more of the cold-worked strength being recovered. The ultimate strength, f_u, followed a similar trend with the quenched and air-cooled samples decreasing in value by 6% and 3% compared with the virgin sample, respectively, whilst the slow-cooled samples increased by 1%. All of the samples examined met the stress ratio requirement $f_u/f_{0.2p}$ being at least equal to 1.08. For the strain response, similar to the samples exposed to 600°C, no distinctive pattern is visible across the three cooling methods. The residual ultimate strain value ε_u increased by 383%-413% against the virgin samples whilst for the failure strain ε_f, the quenched sample had a significant 16% rise, whereas both the air-cooled and slow-cooled samples changed by less than 1%.

After exposure to 800°C followed by the various cooling methods, the pattern in the stress response remains consistent for both the $f_{0.2p}$ and f_u to those discussed before. The quenched sample lost a significant amount of its strength, with the $f_{0.2p}$ and f_u dropping by 37% and 16% to 529.5 N/mm^2 and 792.9 N/mm^2, respectively. The air-cooled samples exhibited lower strength losses of 28% and 15% for $f_{0.2p}$ and f_u, respectively, whilst $f_{0.2p}$ and f_u for the slow-cooled samples decreased the least, reducing by 24% and 13% to 636.4 N/mm^2 and 816.1 N/mm^2, respectively. All of the samples examined met the stress ratio requirement of $f_u/f_{0.2p} \geq 1.08$. For the strain behaviour, the samples exposed to temperatures of 800°C presented the greatest increases against the virgin sample values whilst also presenting a different shape for the overall stress-strain response. The ultimate strain ε_u increased by 2363% from 1.5% to 48.8% for the quenched sample, 2428% from 1.5% to 49.7% for the air-cooled samples and 2168% from 1.5% to 45.9% for the slow-cooled samples. The residual failure strain values ε_f also increased from their corresponding virgin-state values, with increases of 201%, 199% and 188%, respectively, for the quenched, air-cooled and slow-cooled specimens, resulting in a more elongated stress-strain curve. The large disparity between the increase in ε_u relative to ε_f is because of the active dissipation of the cold-worked strength as described before, however a complete dissipation is not achieved, thus resulting in a reduction (or sag) in the stress-strain curve, as seen for all three cooling methods in Fig 10. Essentially, these bars yielded before 10% strain was reached, and then strain hardened until around 50% strain before necking occurred. It is noteworthy that this observation was not evident for the bars that were heated to 900°C, as discussed later.

After exposure to the highest temperature included in this study, 900°C, followed by cooling, the residual $f_{0.2p}$ and f_u values decreased by 49% and 25% for the quenched samples compared to the virgin values, 47% and 22%, respectively, for the air-cooled samples, and 42% and 19% for the slow-cooled rebars. Although all three samples met the stress requirement of $f_u/f_{0.2p} \geq 1.08$, only the slow-cooled sample met the minimum $f_{0.2p}$ requirement of 480 N/mm^2 in accordance with BS 6744 [18]. For the ductility, all of the specimens cooled by any of the three methods exhibited an increase in ε_u and ε_f, and the stress-strain curve also indicated that most of the cold-working in the material was lost during heating and not recovered. As before, the changes in ε_u were most significant as the quenched ultimate strain increased by ε_u 1652%, the air-cooled specimens rose by 1374% and the slow-cooled bars grew by 1234%. The equivalent residual improvements to ε_f were 202%, 181% and 190% of the corresponding virgin values for the quenched, air-cooled and slow-cooled samples, respectively.

In order to specifically compare the influence of cooling rate, Fig. 11 presents all of the stress-strain data from tests on cold-rolled grade 1.4362 duplex stainless steel, heated to a range of values and then cooled by one of the three cooling rates examined. The change in shape that occurred for samples that were heated to 500-700°C and then cooled compared with those that were heated to 800-900°C, is consistent for all cooling rates. It is clear that the cold-working effect that was introduced to the bars during production, was permanently lost at a temperature between 700-800°C. Another observation is that the overall residual strength of the quenched samples was consistently lowest of those tested, followed by the air-cooled specimens whilst the slow-cooled bars regained the greatest proportion of their original strength. In terms of ductility, there is no significant pattern across all three cooling methods and temperature exposure levels. For bars that were exposed to 500-700°C, there was no significant change to the maximum strains recorded, whereas following heating to higher temperatures, as previously discussed, the maximum strains increased significantly, owing to the loss of the cold-working effect. For all bars that were exposed to 600°C and above, the minimum specified requirement of ε_u being at least 5% was consistently achieved [18].

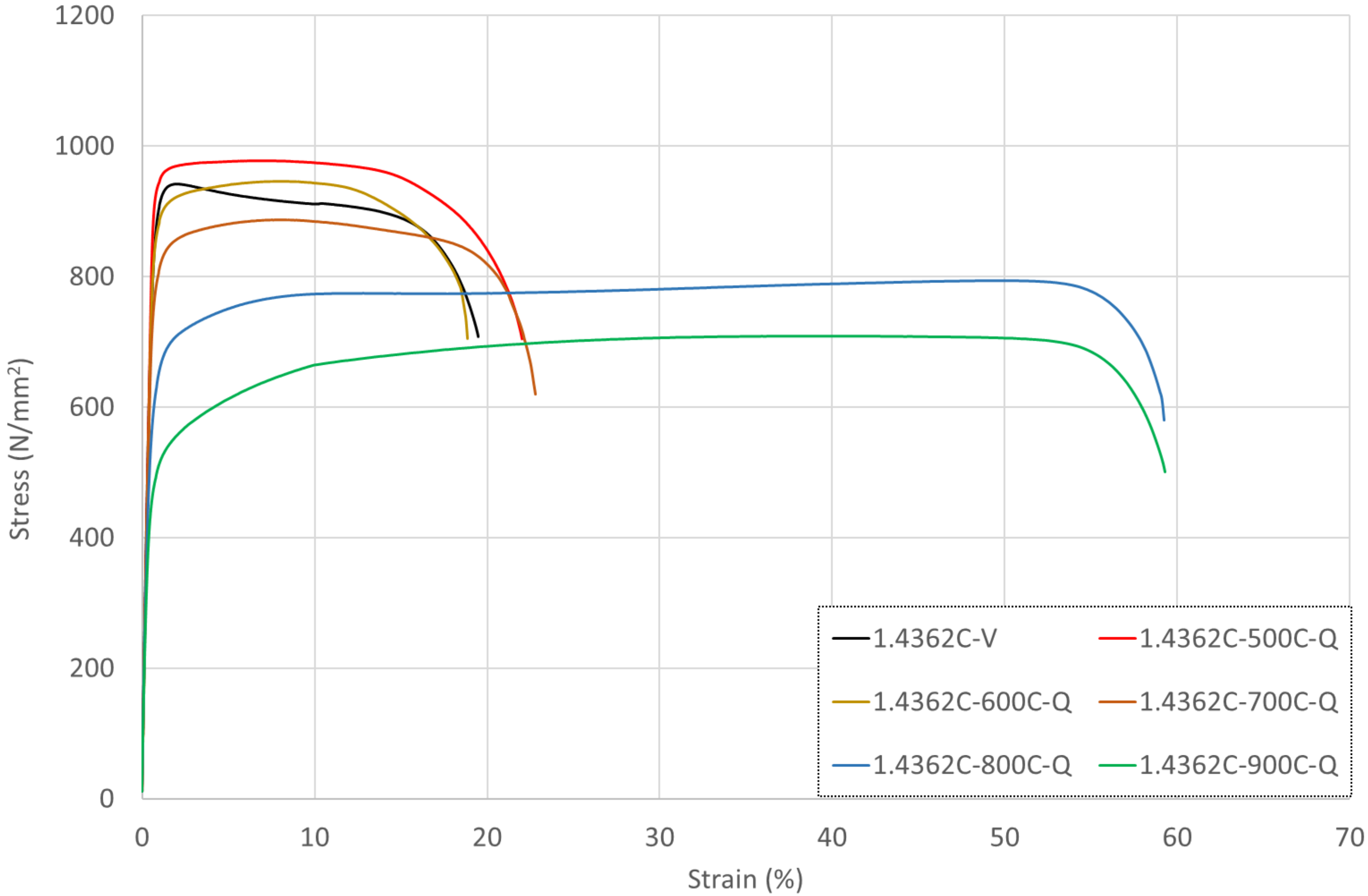

1200
1000
800
600
400
200
0
Stress (N/mm²)
0
10
20
30
40
50
60
70
Strain (%)
1.4362C-V
1.4362C-500C-Q
1.4362C-600C-Q
1.4362C-700C-Q
1.4362C-800C-Q
1.4362C-900C-Q

(a)

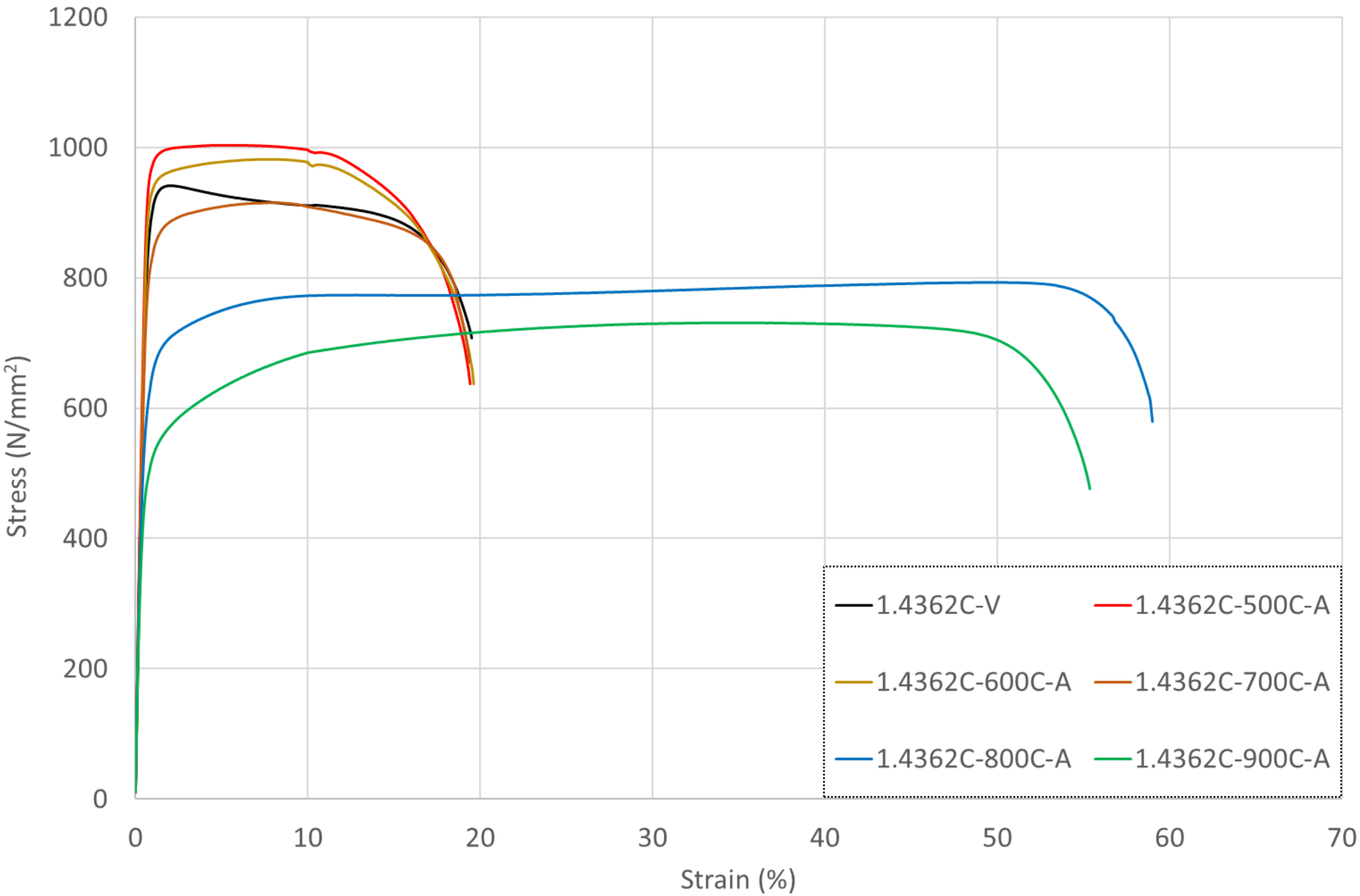

Stress (N/mm^2)
0
200
400
600
800
1000
1200
Strain (%)
0
10
20
30
40
50
60
70
1.4362C-V
1.4362C-500C-A
1.4362C-600C-A
1.4362C-700C-A
1.4362C-800C-A
1.4362C-900C-A

(b)

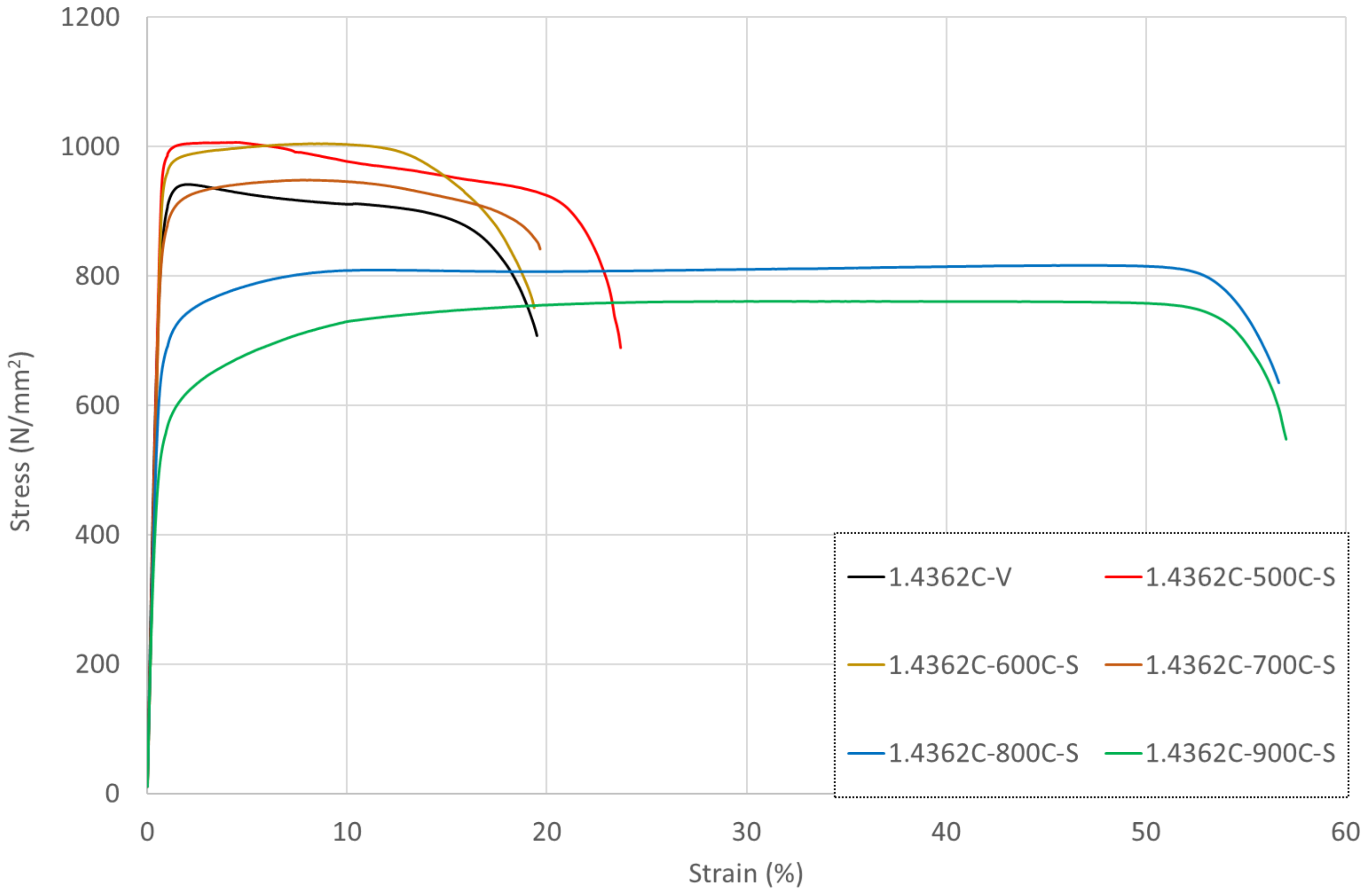

(c)

Figure 10 Stress-strain response for grade 1.4362 cold-rolled duplex stainless steel rebars following exposure to various degrees of elevated temperature and then cooled by (a) quenching in water, (b) naturally, in air and (c) slowly, in the furnace

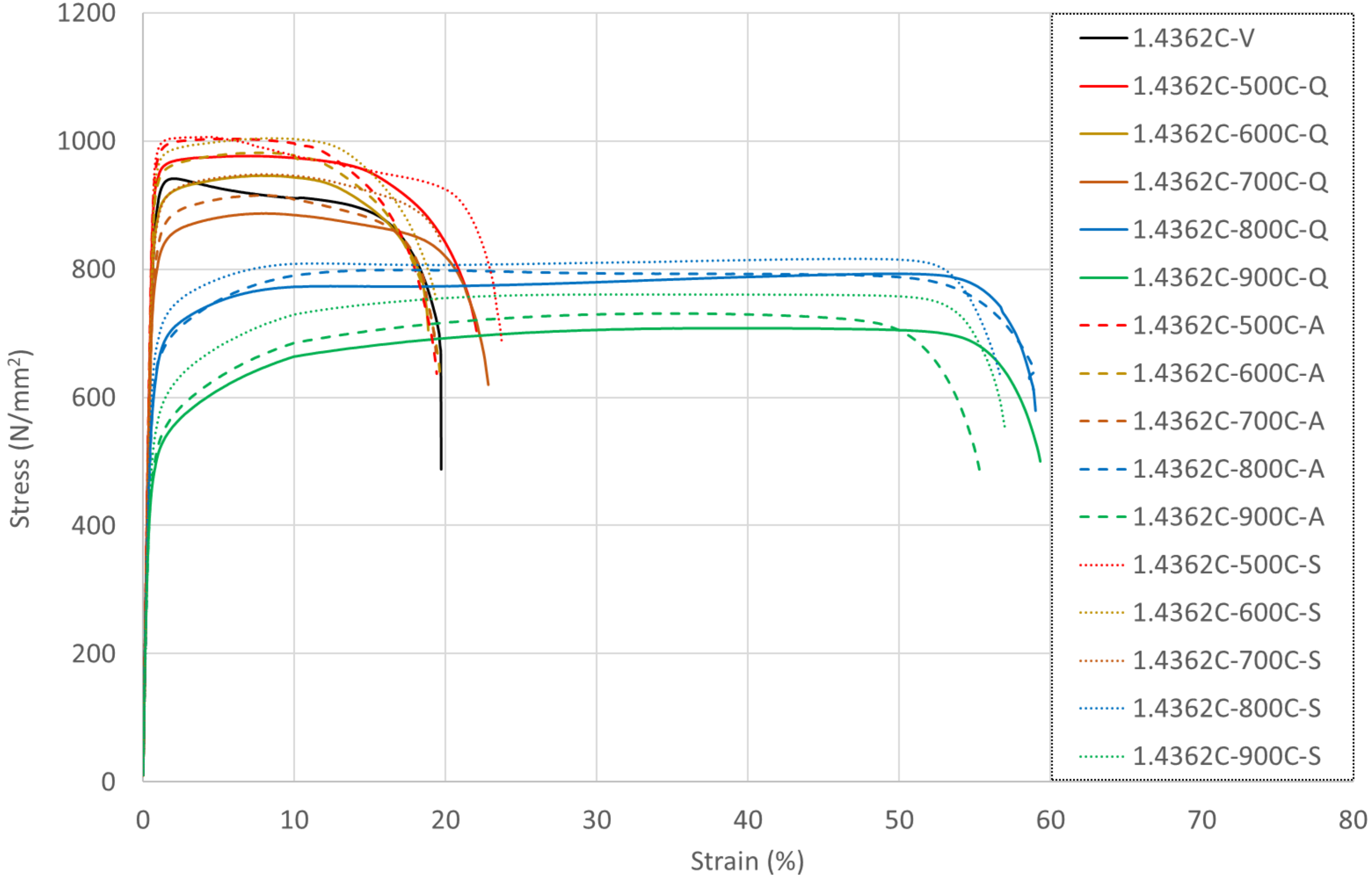

Figure 11 Stress-strain response for grade 1.4362 cold-rolled duplex stainless steel rebars following heating to various temperature before subsequent cooling

6.0 Discussion

Following the detailed investigation of the residual mechanical properties of duplex stainless steel reinforcing bars after exposure to elevated temperature before subsequent cooling, a number of key observations are made. First, regardless of the level of exposure temperature, for the samples cooled quickly through quenching in water, both of the measured strength parameters ($f_{0.2p}$ and f_u) exhibited the least gain in residual properties of the three cooling methods when heated to 500-700°C and the greatest loss following higher temperature exposures. On the other hand, the slow-cooled samples demonstrated the greatest increase in residual strength compared with the corresponding virgin values following exposure to 500-700°C and the lowest loss of strength following exposure to higher temperatures.

The variance in performance following the different cooling methods is due to changes in the internal stresses, particularly in the ferrite grains. During the gradual heating process, which was the same for all specimens, the residual stresses present in the alloy were slowly released. When the alloy was cooled quickly through quenching following elevated temperature exposure, new stresses formed due the sudden temperature reduction and these were retained in the material as residual stresses due to rapid recrystallisation. The presence of residual stresses resulted in poorer performance retention in terms of the post-fire mechanical properties compared with the air-cooled and slow-cooled specimens (for all levels of temperature examined). When the specimens were air-cooled, the alloy cooled at an intermediate rate and, for the samples that were heated to a temperature less than the recrystallization temperature of 727°C, a tempering effect was then produced upon cooling which allowed for the residual stresses to be partially relaxed. This resulted in post-fire properties which were better than the quenched samples but less good compared with the slow-cooled rebars, for all levels of temperature exposure examined. For the bars that were slow-cooled, the phenomenon was similar to an annealing process, with the slowest cooling rate allowing for the gradual growth of new grains and the development of less residual stresses, thus resulting in the highest overall post-fire mechanical property values compared with their quenched and air-cooled counterparts for each examined temperature level.

For the different levels of temperature exposure examined, the results varied greatly between the hot- and cold-rolled samples. For the hot-rolled rebars exposed to temperatures of 500°C and 600°C and subsequently cooled, well-defined yield points were observed in the residual stress-strain curves. These well-defined yield points were the product of an unstable austenitic-ferritic grain boundary. The cold-rolled samples tested under the same conditions presented a more rounded yielding behaviour, typical of stainless steel, with the exception of the cold-rolled sample exposed to 500°C and slow-cooled, which retained more of the original cold-worked properties.

For the samples that were exposed to temperatures of 700°C and 800°C, the hot-rolled duplex stainless steel rebars had good overall retention of their mechanical properties compared with the original values, generally retaining within 15% of the original strength and 25% of the original strain values. For the cold-rolled bars exposed to 700°C , all three cooling methods resulted in a good retention of the original mechanical values. However, as discussed, the slow-cooled sample presented an additional undesirable transformation of the σ phase within the grain boundaries. The σ phase consists of chromium rich zones, which deprive the surrounding area of chromium, effectively compromising the resistance of the alloy towards pitting corrosion. Once the cold-rolled specimens were exposed to temperatures of 800°C and subsequently cooled, regardless of cooling method, the alloy had begun to actively lose the strength induced through cold-rolling. For all samples exposed to temperatures of 900°C and subsequently cooled, a significant loss of strength and increase in strain was recorded, an indication of the grain reverting to γ-austenite. At this stage, most of the strength induced through the heating and cooling process, regardless of the production method, was lost.

Based on the findings of this study, a series of residual strength retention factors for grade 1.4362 duplex stainless steel reinforcing bar are recommended for material that has been exposed to temperatures between 500-900°C. The proposed retention factors are given as $k_{p0.2}$ and k_u which represent the ratio of the 0.2% proof strength and ultimate strength of a given material at elevated temperature, respectively, to the corresponding original values at 20°C. The values presented in Table 5 for both hot- and cold-rolled rebars and are dependent on the cooling rate. Some of the values presented in the table are greater than unity as these property values increased following temperature exposure. In practice, it might not be possible for an engineer to know the cooling rate that occurred. Therefore, Table 6 presents a single set of retention factors which can be applied for any cooling rate safely, based on the findings of the experiments presented herein. These may not be as efficient as employing the values in Table 5, but can be more widely applied when the cooling method is unknown. It is noteworthy that some of the reduction values recommended in Table 6 are different to those previously found [11], as the current work is concerned with reinforcing bar whereas that study focuses on structural sections; the strengthening mechanisms, and degree of cold work, can be quite different during the production process of these two different products.

Table 5 – Retention factors for grade 1.4362 stainless steel reinforcing bar.

	Retention factors for hot-rolled bars		Retention factors for cold-rolled bars	
Temperature exposure level and cooling method	$k_{p0.2}$	k_u	$k_{p0\ 2}$	k_u
Virgin	1.00	1.00	1.00	1.00
500°C-Q	1.30	1.06	1.10	1.04
600°C-Q	1.12	1.00	1.01	1.00
700°C-Q	0.95	0.98	0.88	0.94
800°C-Q	0.86	0.96	0.63	0.84
900°C-Q	0.71	0.89	0.51	0.75
500°C-A	1.31	1.06	1.12	1.07
600°C-A	1.20	1.02	1.09	1.04
700°C-A	1.02	1.01	0.94	0.97
800°C-A	0.95	0.99	0.72	0.85
900°C-A	0.76	0.91	0.53	0.78
500°C-S	1.35	1.08	1.17	1.07
600°C-S	1.23	1.07	1.14	1.07
700°C-S	1.11	1.06	1.01	1.01
800°C-S	1.05	1.02	0.76	0.87
900°C-S	0.82	0.95	0.58	0.81

Table 6 – Retention factors for grade 1.4362 stainless steel reinforcing bar irrespective of cooling rate

	Retention factors for hot-rolled bars		Retention factors for cold-rolled bars	
Temperature exposure level	$k_{p0.2}$	k_u	$k_{p0.2}$	k_u
Virgin	1.0	1.0	1.0	1.0
500°C	1.3	1.0	1.1	1.0
600°C	1.1	1.0	1.0	1.0
700°C	0.9	0.9	0.8	0.9
800°C	0.8	0.9	0.6	0.8
900°C	0.7	0.8	0.5	0.7

7.0 Conclusions

This paper presents a detailed analysis and discussion on the post-fire behaviour of duplex stainless steel reinforcing bar. The data presented includes both mechanical test results as well as a metallurgical assessment. The work was motivated by the previous lack of available data on the behaviour of duplex stainless steel rebars, post-fire, although these are an increasingly popular construction material. In addition, there was a strong desire to provide engineers with the necessary fundamental information so an accurate assessment of the structural integrity of a building following a fire could be made, thus avoiding unnecessary demolition and re-building.

In this paper, the results from over 70 individual tests including 32 mechanical tests and 38 metallurgical tests are presented. A summary of the key findings are given as:

(1) Following exposure to 500°C and 600°C, and subsequent cooling, the hot-rolled samples were compromised through the appearance of the 'yield-like' phenomena, whereas the cold-rolled specimen retained more of the original values.
(2) When exposed to temperatures of 700°C, and subsequent cooling, the corrosion resistance of the slow-cooled cold-rolled samples may be compromised due to the presence of a σ phase in the grain boundary, but all three cooling regimes retained an acceptable level of mechanical response. The hot-rolled samples presented little change, and behaved consistent to the virgin, unheated specimen. It is recommended that the retention of corrosion resistance in duplex stainless steel reinforcing bars following a fire is an area that requires further research.
(3) Following exposure to 800-900°C and subsequent cooling, the cold-rolled reinforcing bars retained a sufficient degree of their original mechanical values to satisfy the criteria given in Part 12 of BS 6744 [18], but also had excessive elongations before failure. This can be also seen for the hot-rolled specimen following exposure to 900°C.
(4) Compared to the cold-rolled specimens, the hot-rolled bars presented greater changes overall in the residual material behaviour following a fire scenario.
(5) The method of cooling influences the residual strength of the material, with slower cooling methods retaining a lower proportion of the original values following exposure to 500-600°C and more of the original values after exposure to higher temperatures.

(6) Consistent instabilities are caused in grade 1.4362 duplex stainless steel rebar between the austenite and ferrite grain boundaries following exposure to fire and subsequent cooling. The volatile grain boundary can compromise the corrosion resistance of the alloy, which is an area that would benefit from further research.

8.0 References

[1] Steel-Sci, “Properties of Stainless Steel Rebar,” 18 05 2021. [Online]. Available: https://www.stainlesssteelrebar.org/stainless-properties/.

[2] Government of Canada, “Pont Samuel-De Champlain - Foire aux questions,” 18 05 2021. [Online]. Available: https://www.infrastructure.gc.ca/nbsl-npsl/faq-fra.html#q1.

[3] worldstainless.org, “Samuel De Champlain Bridge - ISSF Stainless Steel in Bridges,” worldstainless.org, 2019.

[4] worldstainless.org, “River Delta Crossing - ISSF Stainless Steel in Infrastrucutre,” worldstainless.org, 2016.

[5] R. Mondal, A. Rajapgopal, S. Bonagani, A. Prakash, D. Fuloria, P. Sivaprasad, G. Chai, V. Kain and I. Samajdar, “Solution Annealing of Super Duplex Stainless Steel: Correlating Corrosion Performance with Grain Size and Phase-Specific Chemistry,” *Metallurgical and Materials Transactions,* pp. 2480-2494, 2020.

[6] J. L. Cardoso, M. S. Pacheco, A. Araujo and J. Riberio, “Stainless Steel Rebar for Marine Environment: Study of Galvanic Corrosion with Carbon Steel Rebars Used in the Same Concrete Structure,” 2018.

[7] L. Bertolini and M. Gastaldi, “Corrosion resistance of low-nickel duplex stainless steel rebars,” *Materials and Corrosion,* vol. 62, no. 2, pp. 120-129, 2011.

[8] L. Gardner, Y. Bu, P. Francis, N. R. Baddoo, K. A. Cashell and F. McCann, “Elevated tempreture material properties of stainless steel reinforcing bar,” 2016.

[9] F. Rehman, K. A. Cashell and L. Anguliano, “Experimental study of the post-fire mechanical and material response of cold-worked austenitic stainless steel reinforcing bar,” *Materials ,* vol. 15, no. 1564, 2022.

[10] R. Felicetti, P. G. Gambarova and A. Meda, “Residual behavior of steel rebars and R/C sections after a fire,” *Construction and Building Materials,* vol. 23, pp. 3546-3555, 2009.

[11] Z. Tao, X.-Q. Wang, M. K. Hassan, T.-Y. Song and L.-A. Xie, “Behavior of three types of stainless steel after exposure to elevated temperatures,” *Journal of Constructional Steel Research,* vol. 152, pp. 296-311, 2018.

[12] B. A. Pramanik and A. Kumar, Stainless Steel: Microstructure, Mechanical Properties and Methods of Application, Nova, 2015.

[13] J. Beddos and J. G. Parr, Introduction to Stainless Steel, 3rd ed., ASM International, 1999.

[14] International Stainless Steel Forum, "The Stainless Steel Family," ISSF, 2020.

[15] *BS EN 10088-1 Stainless Steel Part 1: List of stainless steels,* British Standards Institute, 2014.

[16] D. G. Rodrigues, G. G. B. Maria, B. A. L. Viana and D. B. Santos, "Effect of low cold-rolling strain on microstructure, texture, phase transformation, and mechanical propeorties of 2304 lean duplex stainless steel," Materials Characterization, 2019.

[17] Danieli Group, "SN Longos reconfirms its confidence in Danieli Rebar-in-Coil Technology," 25 09 2015. [Online]. Available: https://www.danieli.com/en/news/news-events/sn-longos-reconfirms-its-confidence-danieli-rebar-coil-technology_37_18.htm. [Accessed 2021].

[18] *BS 6744:2016 Stainless Steel Bars - Reinforcement of concrete - requirements and test methods,* British Standard Institute, 2016.

[19] L. Twilt, "Strength and Deformation Properties of Steel at Elevated Temperatures," *Fire Safety Journal,* vol. 13, pp. 9-15, 1988.

[20] *BS 6892-1:2016 Metallic materials - Tensile testing, Part 1: Method of test at room temperture,* British Standard Institute, 2016.

[21] Bruker, "The Swiss Army Knife of the X-ray Diffractionist," 2021. [Online]. Available: https://www.bruker.com/en/products-and-solutions/diffractometers-and-scattering-systems/x-ray-diffractometers/diffrac-suite-software/diffrac-eva.html. [Accessed 2021 10 7].

[22] N. Hansen, "Hall–Petch relation and boundary strengthening," *Scripta Materialia,* vol. 51, no. 8, pp. 801-806, 2004.

[23] H. Alinejad and M. Abbasi, "Effects of precipitated phases on the magnetic properties of 2304 duplex stainless steel," *Journal of Magnetism and Magnetic Materials,* vol. 537 , 2021.

[24] A. Dehghan-Manshadi, M. R. Barnett and P. D. Hodgson, "Microstructure evolution during hot deformation of duplex stainless steel," *Materials Science and Technology,* vol. 23, no. 12, pp. 1478-1484, 2013.

[25] *Eurocode 2: Design of concrete structures - Part 1-1:General rules and rules for buildings,* CEN, 2004.

[26] H. William, P. R. G., F. P. Marino and e. al, "Corrosion Corrosion Resistant Alloys for Reinforced Concrete," US Department of Highways , 2009.